Estimation of Ground Reaction Force and Zero Moment Point on a Powered Ankle-Foot Prosthesis

Ernesto Carlos Martinez Villalpando

B.S., Electrical Engineering

Universidad Panamericana campus Bonaterra (2001)

Submitted to the Program in Media Arts and Sciences,
School of Architecture and Planning,
in partial fulfillment of the requirements for the degree of

Master of Science in Media Arts and Sciences

at the

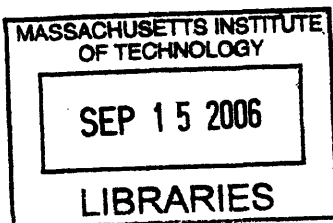MASSACHUSETTS INSTITUTE OF TECHNOLOGY

September 2006

Author: ....
Program in Media Arts and Sciences
August 18th, 2006

Certified by: ....
Hugh Herr, Ph.D.
Associate Professor of Media Arts and Sciences
and Health Sciences and Technology

Accepted by: ....
Andrew B. Lippman, Ph.D.
Chair, Department Committee of Graduate Studies
Program in Media Arts and Sciences

Estimation of Ground Reaction Force and Zero Moment Point on a Powered Ankle-Foot Prosthesis

Ernesto Carlos Martinez Villalpando

Submitted to the Program in Media Arts and Sciences,
School of Architecture and Planning,
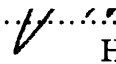in partial fulfillment of the requirements for the degree of

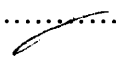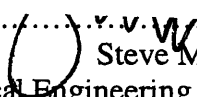Master of Science in Media Arts and Sciences

at the

MASSACHUSETTS INSTITUTE OF TECHNOLOGY

September 2006

Thesis Committee

Research Advisor...
Hugh Herr, Ph.D.
Associate Professor of Media Arts and Sciences
and Health Sciences and Technology

Thesis Supervisor ....
Joseph Paradiso, Ph.D.
Associate Professor of Media Arts and Sciences

Thesis Supervisor ....
Steve Massaquoi, M.D., Ph.D.
Associate Professor of Electrical Engineering and Computer Science
and Health Sciences and Technology

Estimation of Ground Reaction Force and Zero Moment Point on a Powered Ankle-Foot Prosthesis

Ernesto Carlos Martinez Villalpando

Abstract

Commercially available ankle-foot prostheses are passive when in contact with the ground surface, and thus, their mechanical properties remain fixed across different terrains and walking speeds. The passive nature of these prostheses causes many problems for lower extremity amputees, such as a lack of adequate balance control during standing and walking.

The ground reaction force (GRF) and the zero moment point (ZMP) are known to be basic parameters in bipedal balance control. This thesis focuses on the estimation of these parameters using two prostheses, a powered ankle-foot prototype and an instrumented, mechanically-passive prosthesis worn by a transtibial amputee. The main goal of this research is to determine the feasibility of estimating the GRF and ZMP primarily using sensory information from a force/torque transducer positioned proximal to the ankle joint. The location of this sensor is ideal because it allows the use of a compliant artificial foot to be in contact with the ground, in contrast to rigid foot structures employed by walking robots. Both, the active and passive, instrumented prostheses were monitored with a wearable computing system designed to serve as a portable control unit for the active prototype and as an ambulatory gait analysis tool. A set of experiments were conducted at MIT's gait laboratory whereby a below-knee amputee subject, using the prosthetic devices, was asked to perform single-leg standing tests and slow-walking trials. For each experiment, the GRF and ZMP were computed by combining the kinetic and kinematic information recorded from a force platform and a 3D motion capture system. These values were statistically compared to the GRF and ZMP estimated from the data collected by the embedded prosthetic sensory system and portable computing unit. The average RMS error and correlation factor were calculated for all experimental sessions.

Using a static analysis procedure, the estimation of the vertical component of GRF had an averaged correlation coefficient higher than 0.96. The estimated ZMP location had a distance error of less than 1 cm, equal to 4% of the anterior-posterior foot length or 12% of the medio-lateral foot width. These results suggest that it is possible to estimate the GRF between the ground and a compliant artificial prosthesis with a sensor positioned between the knee and the ankle joint. Moreover, this sensory information is sufficient to closely estimate the ZMP location during the single support phase of slow walking and while standing on one leg.

This research contributes to the development of fully integrated artificial extremities that mimic the behavior of the human ankle-foot complex, especially to help improve the postural stability of lower extremity amputees.

Acknowledgments

"Ecce ego quia vocasti me!"

Gracias a Dios y a la Virgen Santísima por su amparo, guía y protección.

Gracias a mis padres , Ernesto y Ana Rosa, y mis hermanas, Ana Fabiola y Sofía, por su incondicional amor.

I would like to thank my advisor Hugh Herr for given me the opportunity to be in the Biomechatronics lab, for all his advice, support and participation in my research.

My gratitude to my thesis committee: Joseph Paradiso and Steve Massaquoi for their guidance that gave shape to this project.

I especially want to extend my gratitude and recognition to all those persons who were an important part of this process:

Samuel Au, for his never-ending aid in every aspect of the research.
Todd Farrell, for all of the assistance provided with the motion capture system and the gait laboratory experiments.
Bruce Deffenbaugh, for his continuous support and encouragement.
Goutam Reddy and Hector Yuen, for his help with Matlab and signal processing.
Andreas Hofmann and Marko Popovic for their help with Matlab and data analysis.
Doug, for the installation of the force platforms.
Ana Fabiola for her help in the design of the images and schematics

To the biomech group members, Ken P., Dan, Hartmut, Max, Waleed, Conor, Ken, Jeff, Chris, Derek, Tesha, Andrea, Andrew, Danielle, Guillermo, Mint, Ben for making a great environment and team.

Table of Contents

List of Figures

9

List of Tables

1 Introduction

Leg prostheses have been available for centuries. However, even in today's highly technological world, there is no prosthesis that includes a mechanism that replicates the functionality of the ankle-foot complex. Commercial ankle-foot prostheses are completely passive while in contact with the ground, and thus, their mechanical properties, such as ankle stiffness, remain fixed regardless of terrain and walking speed. Having passive lower-limb prostheses with a rigid ankle joint and a set stiffness conveys a series of problems for amputees. One of the main problems is maintaining stability (Buckley et al, 2002) while standing and walking. It is not uncommon for amputees to fall due to the lack of ankle joint articulation and control. Deficient stability and other problems such as: decreased walking speed, gait asymmetry and greater metabolic energy cost, motivate the long term goal of developing fully integrated lower-extremity powered prostheses that can mimic the biological behavior of human limbs.

In the fields of biomechanics and humanoid robotics, postural control is critical for understanding bipedal locomotion. In biomechanics, several control strategies have been proposed to understand the dynamics of human balance maintenance (Winter, 1995; Winter et al. 1998; Morasso and Sanguinetti, 2001; Balasubramaniam and Wing, 2002; Popovic, Goswami and Herr 2005). Some of these strategies emphasize the importance of the ankle-foot complex in balance control (Gatev et al., 1999; Morasso and Sanguinetti, 2001; Zhiming, 2004). In the area of humanoid machine control, similar ankle-foot joint control methods have been implemented to maintain the stability of legged robotic systems (Hirai, 1998; Ito, 2002; Erbatur, 2002; Napoleon, 2002). Powerful strategies for balance control in bipedal systems, proposed in both research fields, rely on the knowledge of the ground reaction force (GRF) (i.e. force of interaction between the foot and the ground) and the zero moment point (ZMP) (Vukobratovic et al, 1969). In the study of bipedal locomotion on level ground, the ZMP is the ground reference point that corresponds to the center of pressure (COP). In these control schemes, ankle-foot movements are actively controlled to reposition the ZMP beneath the foot (Vukobratovic et al, 1969). By modulating the ZMP location, the ground reaction

force can effectively be controlled, hence obtaining dynamic balance stability (Popovic and Herr, 2005; Popovic et al. 2005).

Standard measuring techniques for the GRF and ZMP in human subjects are restricted to a laboratory setting, where analysis tools such as video motion capture and calibrated force platform systems are available. Several researchers have investigated how to develop portable, *in-shoe,* gait analysis tools that accurately estimate the GRF components and pressure distribution underneath the feet (Lawrence &Schmidt, 1997; Davis et al., 1998, Savelbert and de Lange, 1999; Barnett et al. 2001, Morris and Paradiso, 2002; Veltink et al., 2005). Similarly, other investigations have focused on determining the location of the ZMP using wearable sensing units (Giacomozzi et al., 2000; Cordero et al., 2004 Zhang et al., 2005). Sensing technologies have also been implemented in prosthetic devices for gait studies and prosthetic assessment (Berme et al. 1976; Morimoto, 1992; Sanders et al. 1994; Sanders et al. 1997; Takahashi et al. 2004);

In the field of humanoid robotics the GRF and ZMP are generally measured with a series of sensors embedded in the feet. These sensors include pressure sensitive transducers, foot switches, strain gage based sensors, force sensitive resistors (FSR) and novel force-torque transducers (Qinghua, et al. 1992; Hirai et al. 1998; Erbatur et al. 2002; Nishiwaki et al. 2002; Kinoshita et al. 2003, Kinoshita et al. 2004). A major drawback for these sensory systems is the rigidity of the feet structures to which they are attached. The stiffness of the feet hinders the ability of the robot to have a more natural and human-like gait.

In the context of postural control, little research has been done in robotic ankle-foot systems and their clinical relevance to amputee mobility (Au et al., 2005; Au et al. 2006). The work presented in this thesis is motivated by the goal of developing the world's first fully integrated artificial extremity that effectively mimics the behavior of the human ankle-foot complex.

The objective of this investigation is to study the feasibility of estimating the ground reaction force (GRF) and zero moment point (ZMP) trajectory, using two prostheses: a powered ankle-foot prototype and an instrumented passive ankle-foot

prosthesis worn by a below-knee amputee. In order to control the active ankle foot prosthesis and record all of the information of the embedded sensors in the passive and active devices, an autonomous wearable computing system was built. This portable computing unit allows further gait analysis in real life environments for healthy and amputee subjects. The information collected in the series of experiments performed is essential for the future implementation of balance control algorithms in biomimetic lower extremity powered prostheses.

The proposed estimation method primarily uses the sensory information from a force/torque transducer positioned between the socket and the socket adapter in both prosthetic devices. Fitting this six-directional force sensor at this location allows the use of a compliant artificial foot to be in contact with the ground. Similar sensing technology is commonly used in bipedal robotics to determine the forces interacting with the ground as well as ZMP trajectory. However, the foot structure of the walking robots is very rigid, hindering their gait. Thus, having a sensor proximal to the ankle joint, raises the question of how precise can the estimations of the GRF and ZMP be given of the compliance of the prosthetic foot, necessary in artificial lower extremities.

In the following chapters a description of the design and implementation of the wearable sensory system is presented. Additionally, the applied estimation methods for the GRF and ZMP values are discussed. The results of the different experimental sessions performed are reported, comparing the accuracy of the estimations with the values provided by standard gait analysis methodologies.

The purpose of the research presented in this thesis is to contribute to the development of human rehabilitation technology, whether it be understanding human ankle-foot biomechanics or the interaction between an amputee and his/her prosthesis.

14

2 Background

2.1. Concept definition

2.1.1. Biomechanics

In 1973, Hay defined biomechanics as "the science that examines forces acting upon and within a biological structure and effects produced by such forces". External forces acting on a system can nowadays be quantified using sophisticated measuring devices or estimations based on calculated models (Nigg and Herzog, 1994). Biomechanical research addresses several areas of human and animal movement, and gait analysis is one of the most important methodologies employed by scientists working in the field.

2.1.2. Gait Analysis

As a general concept gait analysis can be defined as the process of quantification and interpretation of animal (including human) locomotion. In the context of human biomechanics the pattern of human walking is called gait and the method to diagnose it referred to as gait analysis. Quantitative gait analysis provides objective documentation of walking ability and is an important tool in the identification of walking abnormalities. Abnormal gait in humans may reflect compensations for underlying pathologies, or even be responsible for the symptoms. The results of gait analysis have demonstrated to be useful in determining the best course of treatment for patients and permitting developments in rehabilitation engineering (Perry, 1992) (motionanalysis.com).

2.1.2.1. Basic Gait Analysis Instrumentation

Modern human gait analysis uses several instrumentation tools. Among the most important and basic tools required are force measuring platforms and 3D motion capture video systems capable of measuring the fundamental kinetic and kinematic information of the persons in evaluation.

15

Force measurement

Force platforms are clinical tools employed to measure the ground reaction force. These devices consist of a top plate (leveled with the surrounding laboratory floor) separated from a bottom frame by force sensors based on piezoelectric or strain gauge transducers. These plates are capable of accurately measuring the forces that a person exerts on the ground as he or she steps on it during gait. The transducers, situated near each corner, are set orthogonal to the others; providing the vertical load and horizontal shear forces measured in the anterior-posterior and medio-lateral directions, respectively. With additional data processing, alternate to the basic ground reaction force vectors and moments, the center of pressure can be determined (Perry, 1992). Based on the measurements made by the force plates, relevant clinical information can be inferred to treat and diagnose pathological gait (Bontrager, 1998).

Modern 3D video motion capture systems are generally combined with the force plates to determine the forces and moments at the joints, through the use of human modeling and reverse dynamics.

Motion Capture System

Video systems for biomechanical studies use more than one camera to track reflective markers that are attached on identified locations on the person that is under evaluation. These systems can be either passive or active depending on the marker type. Active systems use infrared (IR) light emitting diodes (LEDs) and passive systems use markers covered with retroreflective tape. Highly accurate three-dimensional systems use specialized software to determine the coordinates in space for each marker. With the location of each marker, the software of the system can obtain kinematic information and true 3D motions of the body segments marked. Some vendors incorporate kinetic software that helps compute the net joint moments, forces and powers combining the kinematic and anthropomorphic data with ground reaction force components (Bontrager, 1998).

The measurement of ground reaction force is mainly conducted in a gait laboratory utilizing force measuring platforms. These platforms provide full three-dimensional description of the vector of total force applied by the foot to the ground. This vector is different from the vector commonly known as the "gravity line," which extends vertically from the center of mass (or center of gravity) of a static body. The ground reaction force vector is a "reflection of the total mass-times-acceleration product of all body segments and therefore represents the total of all net muscle and gravitational forces acting at each instant of time over the stance period" (Winter, 1984).
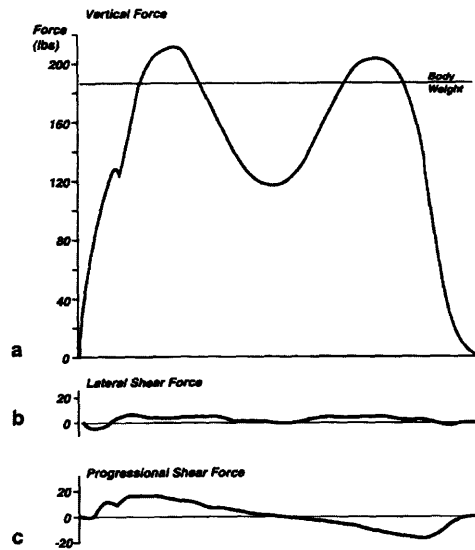
Figure 2-3.Components of the ground reaction force (Perry, 1992)

2.1.4. Center of Mass

The center of mass (CM) of a body or a system of bodies is the point that moves as though all of the mass were concentrated there and all external forces were applied there (Halliday et al., 1997). The CM of an object is the centroid of all mass elements, *dm* with the position vector (Nigg and Herzog, 1994) :

$$r_{CM} = \frac{\int (r\, dm)}{\int dm}$$

18

According to Newton's second law of motion, the sum of external forces acting on a body is equal to the mass of the body times the acceleration of the body's CM.

2.1.5. Center of Pressure

The center of pressure (COP) is a ground reference point where the resultant of all ground reaction forces acts (Nordin and Frenkel, 2001). At this location, it is assumed that all of the forces that act between the body and the ground through the foot (body segment in contact with the floor) can be simplified to a single ground reaction force vector and a free torque vector (www.kwon3d.com)
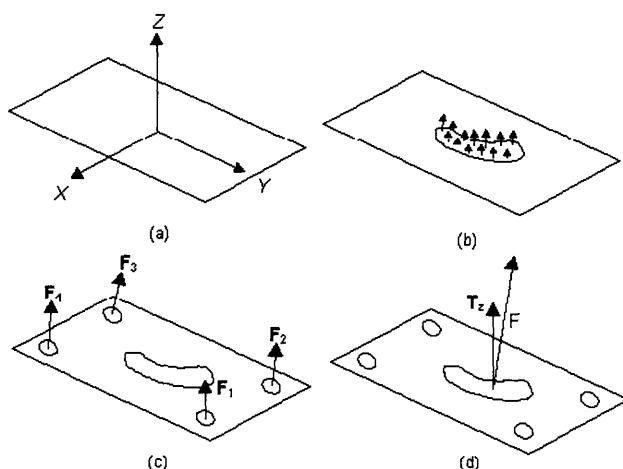
Figure 2-4.Center of pressure when stepping on a force platform. Single ground reaction force **F** and free torque vector Tz . (www.kwon3d.com)

If the horizontal forces between the feet and the ground can be neglected then the center of pressure (COP) can also be defined as the centroid of the vertical force distribution (Elftman, 1934; Cavanagh,1980) or the intercept of the resolved wrench axis with the force plate surface (Shimba, 1984; Soutas-Little 1990).

The position and displacement of the center of pressure during standing and walking provides important clinical insights. It is used to identify abnormal patterns of foot contact, including abnormal toe off or hill strike angle and also helps assess the balancing capabilities of persons.

2.1.6. Zero Moment Point

In the context of legged machine control, Vucobratovic and Juricic (1969) defined the Zero Moment Point (ZMP) as the "point of resulting reaction forces at the contact surface between the extremity and the ground". At any point P under the robot, the reaction can be represented by a force and a moment M_{grf}. Around the ZMP (localized at $\vec{r}_{zmp}$) the moment around the horizontal axis are zero and there is only a component of moment around the vertical axis (Arakawa and Fukuda 1997; Vukobratovic and Borovac 2004; Kudoh , 2004).

$$M_{grf}\left(\vec{r}_{zmp}\right)\big|_{horizontal} = 0$$

$$\text{At } P: \quad M_{grf} = \left(0,0,M_z\right)$$
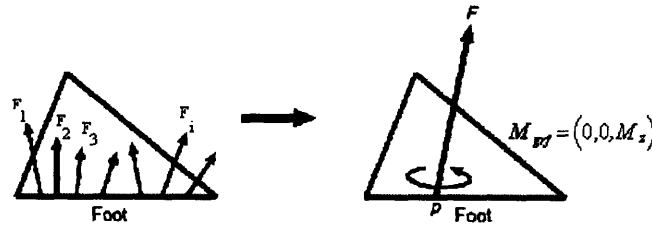
Figure 2-5 Representation of ZMP sagittal plane (Kudoh, 2004).

The resulting moment of force exerted from the ground on the body about the ZMP is always around the vertical axis (parallel to the gravity vector). At the ZMP is a reference point at the ground in which the net moment due to inertial and gravitational forces has no component along the (horizontal) axes (parallel to the ground) (Hirai et al., 1998; Dasgupta and Nakamura, 1999; Vukobratovic and Borovac 2004; Tak, 2000).

For flat horizontal ground surfaces the ZMP is equal to the COP, but are unique in irregular ground surfaces (Popovic et al., 2005). Vucobratovic and Juricic (1969) defined how this point can be calculated from the state of the legged system and its mass distribution. With this point the robotic control system can anticipate future ground-foot interactions from desired body kinematics.

The important notion of the ZMP location is that it resolves the ground reaction force distribution to a single point, and it can be applicable to single and multi-leg support phases of legged systems.

The trajectory that the ZMP follows is utilized to make walking patterns for bipedal walking robots, making it a very important variable for their dynamic balance. These trajectories are planned such that they are within the supporting polygon defined by the location and shape of the foot print (Erbatur et al., 2002). Controlling the ZMP trajectories in the walking robots produces a more natural, human like gait (Park and Rhee, 1998). The motion of humanoid robots can be treated as the relationship between the center of mass and the zero moment point. The ZMP can be also used to determine offline whether certain movements can be done by the robot so it doesn't fall (Kudoh, 2004).

As a natural source of trajectories, human ZMP data is recorded and used as reference for the biped systems. In the detailed study of human ZMP trajectories, Dasgupta and Nakamura (1999) proposed a method to generate reference curves for bipedal machines. These trajectories enhance the robots dynamic stability while standing and walking on flat ground.

2.2. Ambulatory Monitoring Tools for Gait Analysis

The principal accepted clinical tools for biomechanical assessment of human gait are accurate force measurement platforms and 3D optical systems, both installed in a motion laboratory. In this setting, the evaluation of subject mobility performance is limited by the laboratory restrictions. For example, subjects have to step on the force plates avoiding stepping twice on the same platform, in order to make a correct measurement of the total ground reaction force. This situation adds an undesired and sometimes difficult extra limitation to the patients with gait impairments such as amputees. Moreover, the fixation of the force plates allows measuring only one or two steps per experimental trial. This last impedes measuring ground reaction forces and other parameters in common environments for patients, whose evaluations in daily-life

activities will dramatically affect the development of rehabilitation treatments (Veltink et al., 2005).

Several attempts to implement ambulatory systems for gait analysis have been developed to overcome the previously discussed restrictions and/or limitations of the clinical settings. Commercial systems, instrumented insoles and shoes are among the solutions currently available that contribute to the mobile assessment of gait in a non-lab environment.

Modern commercial *in-shoe* systems such as *Pedar*-X © from Novel (www.novel.de), the *F-Scan*® product series from Tekscan, Inc. (www.tekscan.com) and the instrumented insoles of Cleveland Medical Devices, Inc. provide an advance in the study of gait using portable and mobile devices. These products use paper-thin pressure sensor matrices embedded in shoe insoles that measure dynamic plantar pressures between the feet and the shoes during *real-life* situations. Several investigations have compared the abilities of commercial in-shoe pressure measuring systems to accurately quantify vertical force and temporal parameters with measurements from gait lab and force plate measurements (Lawrence & Schmidt, 1997; Barnett, 2001). Previous work has also been developed to determine the pressure distribution in prosthetic interfaces, and for the measurement of the force and pressure distribution on the plantar surface of the feet (Williams et al., 1992; Davis, et al., 1998)

Even though the in-shoe systems previously discussed allow the estimation of the vertical component of the ground reaction force, they have a major draw-back, which is the lack of direct quantification of the medio-lateral and anterior-posterior forces. Razian & Pepper (2003), investigated the development of an in-shoe triaxial pressure measurement transducers based on piezoelectric film components in order to simultaneously measure shear and vertical forces during gait. Estimation of the full vector of the ground reaction force vector has been investigated by several authors. Savelberg and de Lange (1999) employed artificial neural networks to obtain the horizontal and anterior-posterior components of the ground reaction forces using pressure sensitive insoles. Artificial neural networks have also being used by the investigations of Zhang et al. (2005), using a new mobile device to record and

measure foot-ground force interaction by using an instrumented insole and portable electronics.

Instrumented insoles commonly do not consider the GRF under the foot but just the interaction forces between the foot and the shoe (Giacomozzi et al., 2000; Cordero et al., 2004). In these investigations the use of 3D motion capture systems and force platforms were used to validate their estimation methods using commercial insoles.

Other approaches to develop ambulatory measurement systems to determine the ground reaction forces have been to instrument shoes or foot orthoses. A portable system consisting of an ankle-foot orthosis with mounted force sensitive resistors (FSR's) used by Ferencz et. al. (1993) was used to help estimate the center of pressure during gait for healthy walking individuals. Further work developed by Morris & Paradiso, (2002) includes a shoe-integrated sensor system to continuously monitor and analyze gait wirelessly and in real-time. This system provided information about the three-dimensional motion, position and pressure distribution of the foot in real-time, using complex pattern recognition and numerical analysis of the transmitted data.

The use of a six-axis force sensing footwear for gait analysis was investigated by Takahashi, et al. (2004). This system utilizes a strain-gage force transducer, used in humanoid robots, attached to prosthetic feet. The sensor is interposed between the foot and an ankle-foot orthosis for each foot. With this system the subject straps his feet to the instrumented orthoses/prostheses and walks on them (similar to walking on stilts) while recording data. The results compared the influence of this system in walking and evaluated its capacity to be used as a clinical tool.

Other researchers have proposed the use six-axis transducers implemented in normal shoes as a tool for gait studies. Veltink, et al. (2005), proposed the use of two six-axis force sensors underneath common shoes to enable the ambulatory measurement of ground reaction forces and center of pressure. Their experimental results illustrated the feasibility of such approach in healthy subjects.

All of the previous instrumented systems have been validated by comparing it with to standard and known clinical methods. These methods generally consist of a high definition 3D optical system and a series of force plates within a motion laboratory setting.

Although these systems are contributing to address and treat foot, gait and posture related disorders, limited investigations that include ankle-foot prostheses has been done (Pitkin et. al. 1999, 2002). A major problem when using these portable systems is the fragility of the pressure mat when interacting with the continuous high forces between the rigid artificial foot and the shoe. For long-term usage and implementation on commercial foot ankle-prostheses a distinct instrumentation approach is investigated in this thesis.

2.3. Amputee Gait Abnormalities

The use of gait analysis to determine the treatments of abnormalities during walking has been a main area of research for several years. Gait abnormalities are mainly caused by a physical malfunction. One major cause of dysfunctional gait is due to trauma and amputation of one or both of the lower limbs at different levels. In order to compensate for abnormal patterns due to amputation, prostheses that partially substitute the missing limb function are use as treatment.

Lower limb amputations regularly occur at three levels:

a) Transfermoral amputation- Above knee (AK).
b) Transtibial amputation - Below knee (BK).
c) Amputation at the level of the ankle - Syme's.

For above knee amputees one of the major problems is the coupling between the residual limb and the prosthetic leg. A main reason for this obstacle is the relative motion between the socket and the femur stump caused by the compression of the soft tissue. This motion is uncomfortable for the amputee and causes a lack of confidence to apply large forces to the prosthetic leg. In addition, the relatively short moment arm

between the hip joint and the socket reduces the force that the hip muscles can apply to the artificial limb (Whittle, 1991).

A major cause of modified gait for transfemoral amputees is the need to walk with the knee in full extension during single stance support, since they cannot oppose to an external flexion torque around the knee axis. To prevent this, passive artificial knees with higher stiffness are generally employed. The inconvenience with higher stiffness in the knee joint during the stance phase is that the location of the center of gravity is dramatically affected, increasing the energy needed to walk. Although amputees adapt to this circumstance, this type of walking is energetically demanding for all of patients (Whittle, 1991).

A source of pathological gait for above knee amputees is lack of accurate control of the knee joint during the swing phase. During this phase, the knee cannot be totally free because it will extend too rapidly with a sudden stop hitting the boundary in hyperextension. In contrast, the knee joint cannot be too rigid that it doesn't permit flexion or extension; this will result in an increase of the amount of energy required by the hip muscles to move the prosthesis as a single piece. To prevent these extreme cases, several prosthetic knees that behave as a damper have been developed using friction mechanisms, hydraulic or, pneumatic or electronically controlled systems. Some have been designed as variable damping coefficient depending on the angle, speed and direction of motion. These mechanisms have partially solved some of the problems associated with abnormal gait patterns in amputees (Whittle, 1991).

For below the knee amputees the lack of the ability to articulate their ankle joint generates an abnormal gait. Losing the capacity to actively plantarflex at the end of the stance phase of walking avoids having a powered push off, thus creating the need of lifting the leg sooner to clear the ground, since the effective length of the leg is reduced compared to a normal limb. There are some commercial prostheses that have a spring-like behavior that help store some energy during hill strike and stance phase and releasing it at toe-off. Even though these prostheses have certain compliance and help function as initial and terminal rockers due to their shape, they are still not functional enough to replicate normal ankle's flexibility and actuation (Whittle, 1991).
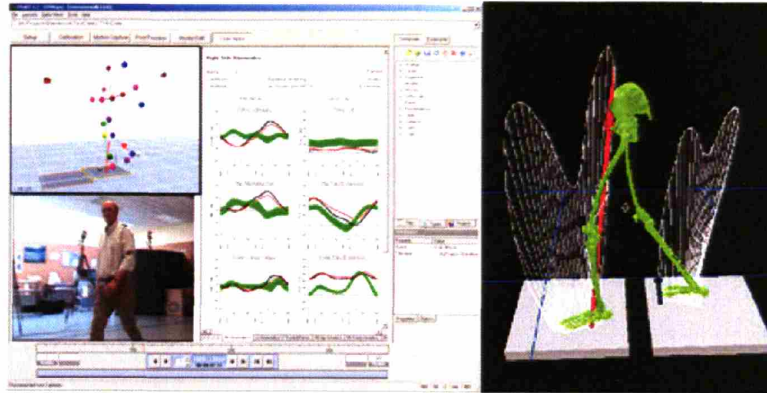
Figure 2-1. Motion analysis using 3D video capture system in combination with force plate data (source: www.motionanalysis.com and **www.vicon.com**)

2.1.3. Ground Reaction Force

As a person stands, walks or runs, there exists constant interaction between the body and the ground. During this interaction, the body weight drops onto and moves across the supporting foot, generating vertical, horizontal and rotary forces on the floor. In accordance to Newton's third law of motion, there is a reaction force supplied by the supporting surface, called the ground reaction force (GRF), which is equal in magnitude and opposite in direction to the force that the body exerts on the supporting surface through the weight-bearing limb (Perry, 1992).
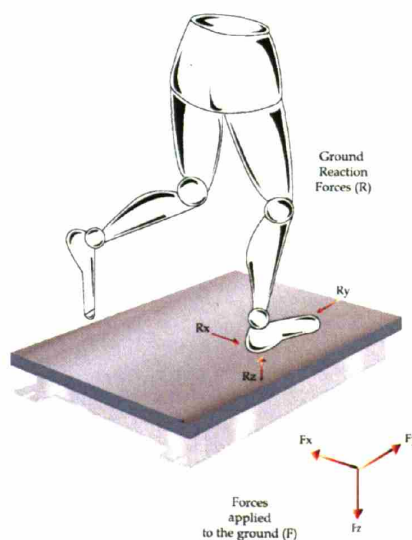
Figure 2-2. Ground reaction force

For a transtibial amputee the hip and the knee in combination compensate in great percentage the lack of the ankle articulation, making the path of the center of gravity is relatively normal (Saunders et al.1953).
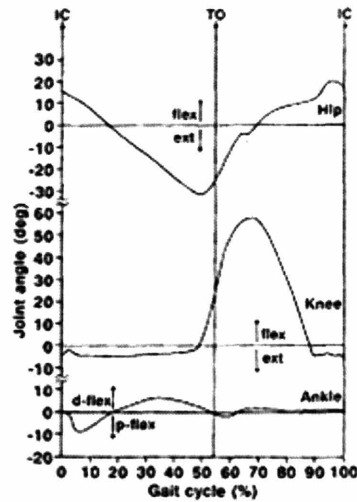
Figure 2-6. Sagittal plane hip, knee and ankle angles during walking in an AK amputee. Abnormality: hyperextension of the knee from before initial contact to just before toe-off (Whittle,1991)

a)   b)
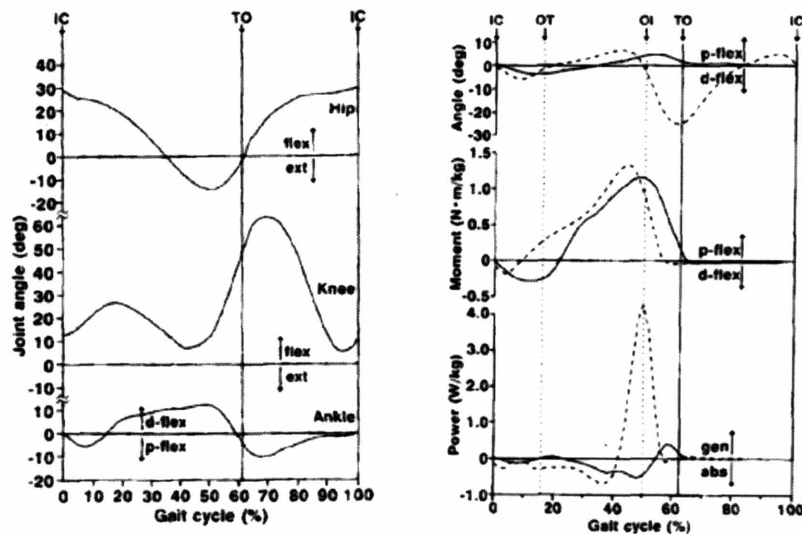
Figure 2-7. a)Hip, knee and ankle angles during walking in below knee amputee. b)Sagittal plane ankle angle, internal moment and power in a transtibial amputee (solid line) and normal subject (dashed line)(Whittle,1991)

A main problem that lower-limb amputees have is a limited balance performance. Buckley, et at. (2002), observed that amputees had poorer static and dynamic balance than able-bodied controls. In this study, amputees spent significantly less time in balance than able-bodied subjects. Amputees had greater problem controlling their dynamic balance in the anterioposterior and mediolateral planes. Their findings "highlight the importance of the ankle in maintaining balance in situations that involve body movements in the sagittal plane".

In the study done by Miller and Deathe, (2004), lack balance confidence was a persistent problem in the lower limb amputee population. In this study, they assessed how balance confidence scores changed over a two year follow up period. They identified predictor variables for balance confidence, suggesting them as important variables that can influence the balance performance of amputees during standing and walking.

Other main changes in below the knee amputation patients compared to normal subjects gait are (Whittle, 1991; Klute et al. 2001), :

- Delayed foot flat.
- Reduced stance phase knee flexion.
- Early heel rise.
- Early toe off.
- Reduced stance phase duration.
- Reduce swing phase knee flexion.

2.4. Humanoid Robotics

In the past few years, research in humanoid robotics has become a field of great interest for the scientific community. The anthropomorphic characteristics have made of the robotic bipedal systems the most versatile structures to move and walk in complex human environments. These systems present advantages over wheeled vehicles, specifically in obstacle avoidance and locomotion. Nevertheless, the complexity of control of such machines is a challenge. The sensing of the ground

reaction force and zero moment point trajectory are important criteria for stability and walking control of these systems, which a number of researchers have investigated.

A method to determine the location of the zero moment point (ZMP) in bipedal robots is to use direct sensory information of transducers inserted underneath the feet of the robots. A variety of sensors to determine the ZMP location have been used by researchers; these include: six degree of freedom force-torque transducers, pressure sensitive sensors, polymer film devices, load cells and other strain-gage based sensors. Erbatur et al. (2002) used ZMP sensors based on force sensitive resistors (FSR) in two biped robots and compared their ZMP curve results to human ZMP trajectories.

Force torque transducers with one or several degrees of freedom have been also implemented in walking robots to measure the ground reaction force and estimate the zero moment point trajectories. Qinghua, et. al. (1992) used a universal force-moment sensor to determine the ZMP in their biped robot. A six-axis force sensor with parallel support mechanism was proposed by Nishiwaki, et al. (2002) to measure the ground reaction force vector and the ZMP trajectory for the Japanese humanoid robot *H7*. Humanoid robots such as Honda's ASIMO also employs a six-axis force transducer to sense the ground reaction force and to use it to estimate the location of the ZMP (Hirai, et. al. 1998).
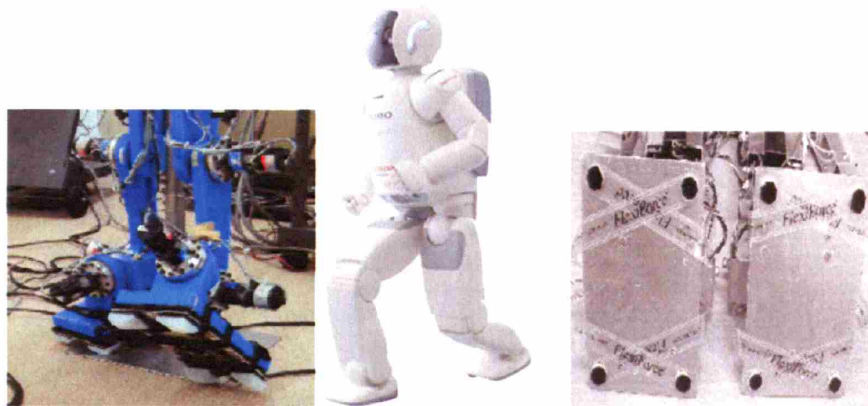
Figure 2-8. Sensors underneath robot feet to measure GRF and ZMP
(source:http://www.kawalab.dnj.ynu.ac.jp/robot_index/robotics_at_KawaLab_j.html,
http://www.honda.co.jp/ASIMO/)

Another approach to determine the ground reaction force distribution on the sole of a walking humanoid robot (HOAP-1) was proposed by Kinoshita et. al. (2003). In their investigations they propose a tactile array sensor for the sole of the robot feet, using conductive rubber. In their approach similar technology like the commercially available pressure insole developed by Tekscan ® was implemented, allowing measuring the pressure distribution when stepping on uneven surfaces.

A primary consideration in bipedal robots is balance maintenance. Robots use different sensors that resemble human sensory sources for balance maintenance:

- Body Linear acceleration is sensed by the otolith in the inner ear is replaced in robots by accelerometers.
- Angular speed sensed by semicircular canals in humans has its technological counterpart represented in gyroscopes.
- Sensory information from the muscles and skin, that *inform* the operating angle of joints, angular speed, power and pressure on the feet soles and skin sensations is replace in robots by force-torque transducers and joint angle sensors.

A powerful method for balance control in bipedal robots is based on the ZMP criterion (Vukobratovic, et. al. 1969). The planned and programmed motions should be such, that this reference point exists under the foot and support polygon during locomotion, avoiding the fall of the robot. A number of researchers have developed several methods for balance control of bipedal systems that consider the use ground reaction force and ZMP trajectory (Ito and Kawasaki, 2000, 2003; Napoleon et. al. 2002; Goswami and Kallem, 2004; Hoffmann et. al. 2004).

In lower limb amputees the capacity of sensing the pressure distribution underneath their feet is lost. In the present investigation the use of sensing technology, currently employed in bipedal system is integrated into a robotic ankle-foot prosthesis. It is the intention to merge sensing methods used in humanoid robot technology and evaluation procedures in human biomechanics to establish the basis to develop an active ankle-foot prosthesis capable of compensating for amputees' postural control difficulties during standing and walking. Based on the theory of human balance and

29

postural control strategies, active ankle controllers can be implemented in the powered ankle prostheses. These devices can then *intelligently* work in parallel with the amputee to improve his/her posture and walking efficiency to levels similar to healthy subjects.

3   Hardware Description

3.1. Experimental Apparatus

For this investigation two types of prostheses were employed: commercial ankle-foot prosthesis (LP Variflex ® from Ossur©) and an active prosthesis prototype developed by the Biomechatronics group of MIT's Media Laboratory. Both devices were instrumented with several sensors in order to estimate the ground reaction force vector and the trajectory of the ZMP.

The main hardware components used for the experiments are enumerated and described in the following sections:

1. A commercially available ankle-foot prosthesis
2. An active ankle- foot prototype
3. Instrumentation sensors
4. A wearable computing system
5. Vicon® 3D motion capture system
6. AMTI® force plate system

3.1.1. Passive Ankle Foot-Prosthesis

The commercial ankle-foot prosthesis instrumented in this research was a LP Vari-Flex® designed for transtibial amputees by Ossur ©. This prosthesis will be a basis of comparison for the active ank-foot prototype, when the estimation methods are applied on both devices. This prosthesis will also help evaluate how does the compliance of the artifical foot affects the estimations of the GRF components and the ZMP.

The artificial foot mainly made of composite materials (e.g. carbon fiber) with leaf spring structures that have a spring-like behavior with certain stiffness The properties of this foot prosthesis are intended to substitute the loss of muscles and

tendons of the intact biological limb.Although limited, the energy storage-return and stiffness characteristics try to approximate the values for normal human ankle at slow walking speeds (Klute et. al., 2001)

Figure 2-9. Passive Ankle foot prosthesis from Ossur ©: LP Vari-Flex ® and Vari-Flex ®

Commercial passive ankle prostheses present several problems for lower limb amputees, such as decreased gait symmetry, reduced knee flexion during level walking, delayed achievement of the stable foot flat and lack of balance control during standing and walking. Some of these abnormalities can be overcome with a robotic ankle-foot device, capable of controlling the joint position and stiffness. In particular, the lack of balance control can be treated if implementing ZMP trajectory tracking control strategies, similar to the strategies used in bipedal robotics.

3.1.2. Powered Ankle-Foot Prototype

The second device used in this investigation was an active ankle-foot emulator prototype, developed at the Biomechatronics research group of the Media Lab. Based on ankle-foot walking biomechanics; this powered active-ankle foot prosthesis is the first prototype of its kind in the world. The objective of this biomimetic prosthetic device is to behave like a normal human ankle-foot, providing power and varying stiffness depending on walking speed and gait phase of the person. With this technology it will be possible to provide a more natural gait and normal levels of energy expenditure of below knee amputees (Au, Dilworth & Herr, 2006). In addition, the instrumentation of this device will serve as an ambulatory system for gait analysis of amputees, contributing to the understanding of human ankle-foot biomechanics and control. Moreover, identifying parameters such as GRF and ZMP will support the implementation of the active control schemes in the ankle joint that mimic biological behaviors, such as varying stiffness control for postural and balance maintenance.

Figure 2-10. Powered ankle-foot prototype in development at MIT's Biomechatronics research group at Media Laboratory

3.1.2.1. *Design specifications of active ankle* :

Based on the biomechanical descriptions of the human ankle during level-ground walking, specifically on the sagittal plane, the design specifications for the active ankle foot prosthesis developed at the Biomechatronics group were established.

According to Inman, Ralston & Todd (1981), a level ground walking gait cycle can define its start with the heel strike of one foot and its end when at the next heel strike of the same foot. This cycle can be decomposed by two main phases: stance and swing. The stance phase begins at heel strike and ends when the toe of the same foot loses contact with the ground surface (toe-off), and the swing phase is the portion of the cycle when the foot is off the ground after toe-off until heel strike.

Considering the ankle function characterization by Palmer (2002) and Gates (2004), the stance phase can be divided into three more sub-stages:

a) Controlled plantarflexion (CP) : begins at heel strike and ends when the foot is flat on the ground surface.

b) Controlled dorsiflexion (CD): begins the foot is flat on the ground and continues to the maximum point of ankle dorsiflexion (turning of the foot's dorso towards the shank).

c) Powered plantarflexion (PP): begins after controlled dorsiflexion and ends when the toe is off the ground surface. In this stage additional energy is supplied during late stance, along with the energy stored in the ankle-foot structure during dorsiflexion.
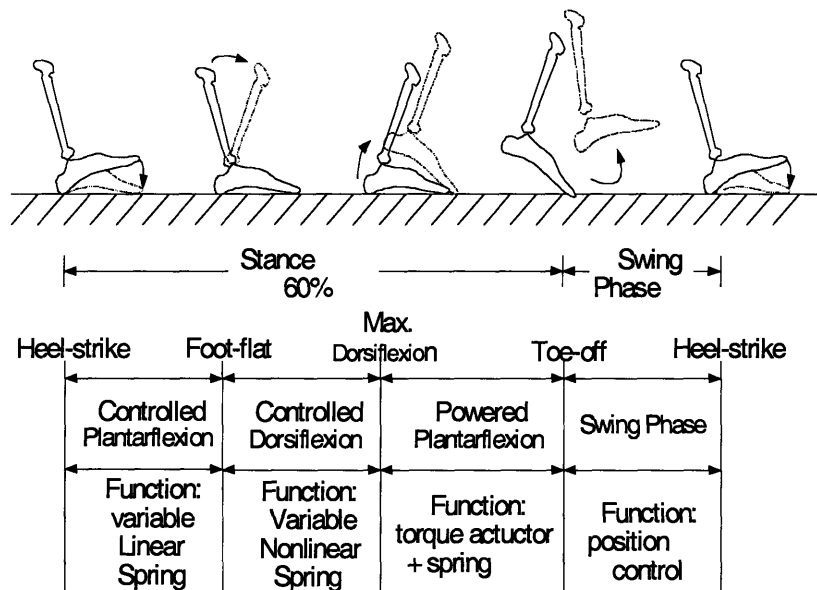
Figure 2-11. Level-ground walking gait cycle phases (Au, Dilworth & Herr, 2006).

34
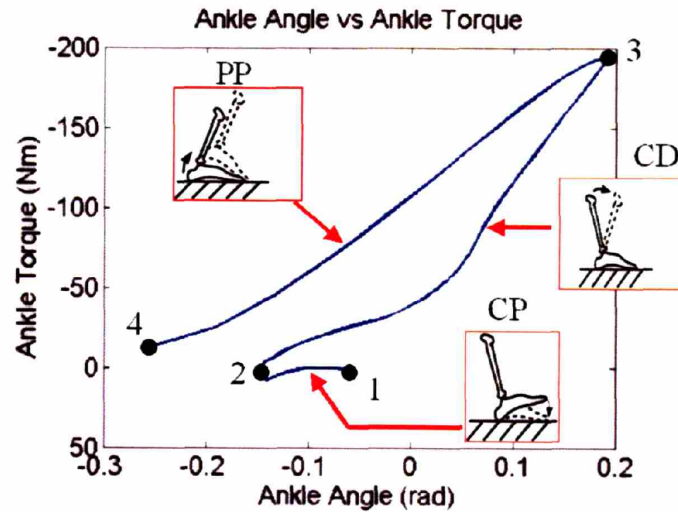
Figure 2-12. Characteristic ankle torque versus ankle angle during level-ground walking. Ankle torque-angle during sub-phases CP, CD, PP are represented in segments 1-2, 2-3,3-4. (Au, Dilworth & Herr, 2006)

With the above behavior description of the ankle-foot joint during level-ground walking, the main specifications for the powered ankle-foot prosthesis proposed by Au et. al. (2006) include:

a) Based on Palmer (2002) a large instantaneous power output power and torque should be provided by the ankle-joint.

b) Variation of stiffness according to the corresponding phase of gait

c) Ankle articulation position control during swing.

	Peak Ankle Power	Peak Ankle Torque	Peak Angular Velocity
Normalized Human Ankle Response	4 W / Kg	1.7 Nm / Kg	5 rad/ sec at 0.25 Nm / Kg
Approximate values (75 Kg person)	300 W	127.5 Nm	5 rad / sec at 18.75 Nm / Kg

Table 2-1. Human ankle joint behavior (Au, Dilworth & Herr, 2006)

3.1.2.2. Mechanical design:

The active ankle-foot prosthesis is comprised of five main elements:

a) High power output DC motor (Maxon® RE-max 40)
b) Transmission (motor gear-head and belt driven system)
c) Series springs
d) Carbon composite prosthesis foot (Ossur© flex foot)

The first three components of the system make a rotary Series-Elastic Actuator (SEA) whose function is to imitate the behavior of the healthy ankle articulation. The parallel springs support part of the loading during different walking gait speeds so that the actuator can provide the instantaneous power required in the design specifications. The carbon composite structure is a commercial device that resembles the function of the human foot.

The Series Elastic Actuator (SEA), technology originally developed at MIT Leg laboratory for walking robot actuation, consists of a DC motor in series with a set of springs to provide series elasticity (Pratt and Williamson, 1995). By measuring the deflection of the springs, force control on the SEA can be obtained. Several advantages make of the SEA an adequate actuator for human interaction in rehabilitation and augmentation applications. Among these advantages we can enumerate the following:

1. Low impedance
2. Isolation of motor from shock load
3. Spring filtered effects of backlash, torque ripple and friction

The transmission has two components: a gear-head coupled to the DC motor with a gear ration of 74:1 and a belt driven transmission to a linear ball-screw system that provides the force necessary to articulate the ankle joint. This system provides a stall torque of 350 Nm and a maximum angular velocity of 5 rad/sec at 25 Nm (Au, Dilworth & Herr, 2006).

36
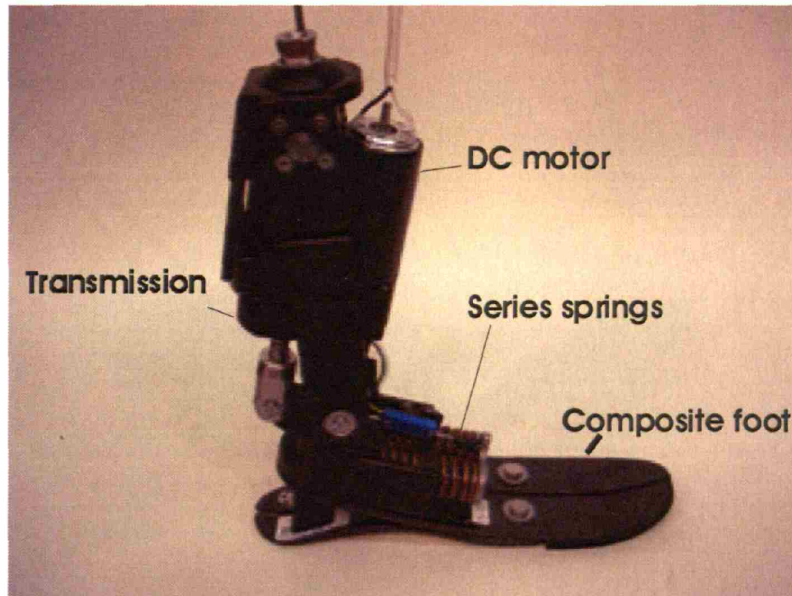
Figure 2-13. Main components of the powered ankle-foot prosthesis prototype

3.2. Instrumentation

Both ankle foot prostheses previously discussed were instrumented with a six degree of freedom transducer installed in the between the amputee's socket and socket adapter the artificial ankle prostheses (proximal to the ankle joint). This six-directional transducer is capable of measuring three force components and three moments, generated by the forces interacting with the ground. Additional sensors were implemented in the active ankle prosthesis to measure values of angle and torque of the artificial ankle joint, as well as temporal parameters of contact with the ground. From the information of these series of sensors the GRF components and ZMP location were estimated.

3.2.1. Ankle Torque Sensor

The torque around the ankle joint is measured indirectly with a linear potentiometer of 5 KΩ (Bourns 3048), installed across the flexion and extension springs that are in series with the DC motor. As force from the SEA actuates the ankle joint the springs suffer a deflection or compression which is measured be linear variable resistor.
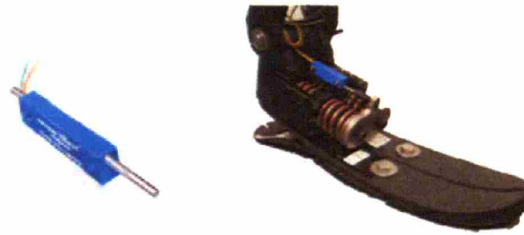
Figure 2-14. a) Bourns© linear potentiometer. b) Potentiometer installed across series springs

3.2.2. Signal Conditioning Board

To reduce the noise levels in the signal from the linear potentiometer that represents the ankle torque, the voltage signal was amplified with a differential line driver and then filtered with an analog low pass filter with a cut off frequency at 1.5 KHz. Once conditioned, the amplified and filtered signal is sent to a specific breakout board which is read by a data acquisition system on a wearable computing system.
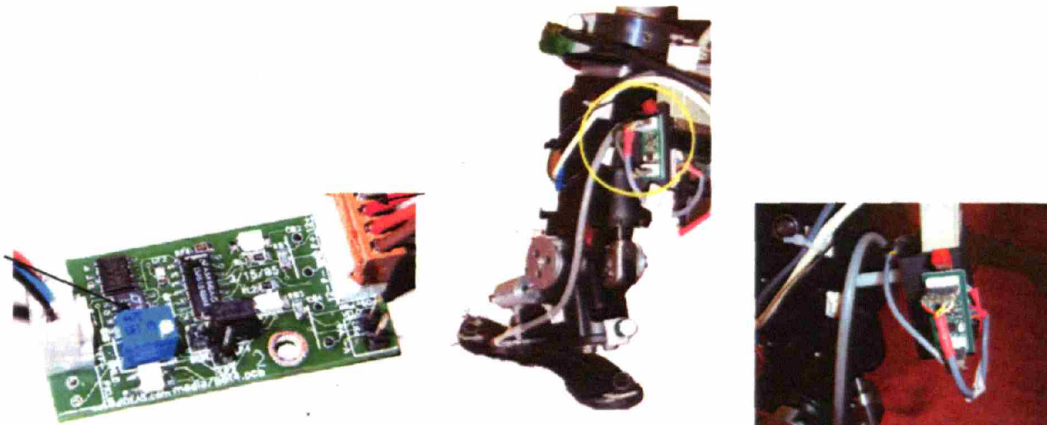
Figure 2-15. Signal conditioning PCB and its location in the active ankle-foot prosthesis

3.2.3. Ankle Angle Sensor

In order to determine the position of the ankle joint a 500-line quadrature encoder module (US digital, Inc. HEDS 9140) was employed. The enconder was mounted in the axis of the ankle joint between a *parent* link plate (the shank structure) and a *child* link plate (part of the foot structure).

a)   b)
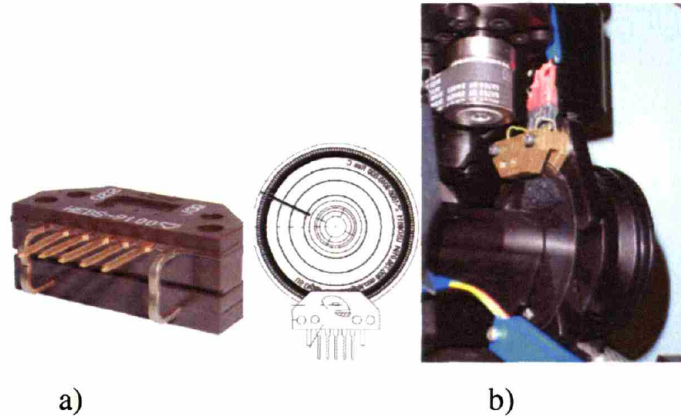
Figure 2-16. a) US Digital © 9140 encoder and b) Encoder mounted at the ankle joint

3.2.4. Floor Contact Sensors

A series of six force sensing resistors ® (Interlink Electronics No. 402) were embedded underneath the carbon composite foot prosthesis of the active ankle in order to detect when the foot makes contact with the ground. Two of the sensors were mounted on underneath the toe area, two in the metatarsal zone and two more on the hill of the leaf spring structures. These sensors were employed as variable force threshold switches. Initially, a specific circuitry was used to transmit on / off conditions of the switches. The electronics were simplified using the analog to digital (A/D) conversion capabilities of the computing unit used for the experiments. This simplification eliminated the use of a specific comparator operational amplifier. The purpose of these sensors is to determine temporal parameters during stance and gait experiments conducted during this investigation.

a)   b)
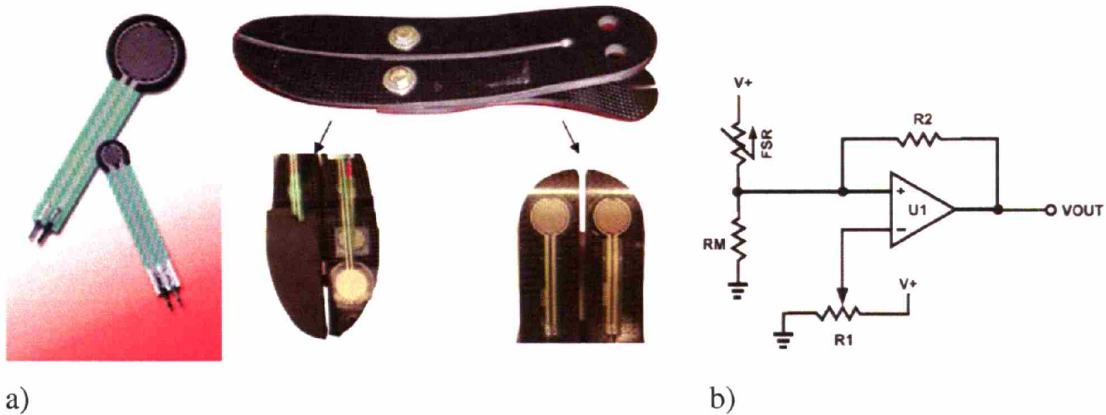
Figure 2-17. a) Interlink FSR® technology used as a variable force threshold switch mounted on carbon composite foot. b) Initial circuit schematic for variable force threshold switch detection.

3.2.5. Ground Reaction Force Measuring Systems

Diverse measuring systems to measure the ground reaction force and temporal parameters were investigated:

a)   *Matrix-based pressure sensing systems*:

1. A matrix array for an in-shoe insole (F-Scan®) with 960 sensing points from Tekscan® . This flexible tactile force sensor in a grid configuration requires a connection to a "handle", which is a breakout box with a connetion to the computer to transmit the sensor data. Specific PC software from the company is required to process the data and cannot be used for real-time control applications.
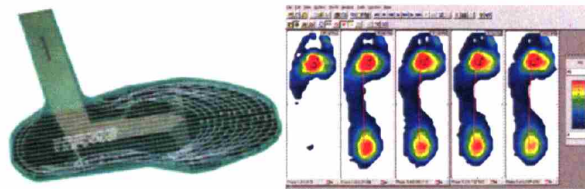
Figure 2-18. Tekscan® F-Scan System.

2. Capacitance force transducers. From Novel electronics, the system Pedar-X uses a matrix of multiple capacitance transducers embedded in an insole with 256 sensors in each foot. Similar to Tekscan technology a "handle" is required to process the raw data to a PC usable format, where a specific software developed by the company is required to obtain the desired information.

Figure 2-19. Novel® Pedar-X insole

b) Discrete switch insole

Initial research for a multiple switch discrete insole to determine temporal parameters during gait was realized. A custom made insole with 24 distributed copper switches was proposed to determine locations of contact under the foot (healthy and prosthetic) during interaction with the ground. This insole had a reduced accuracy and repeatability.

Figure 2-20. Custom made discrete switch insole.

c) Six-axis load cell

A multi directional force-torque transducer was selected to measure the interaction forces between the prostheses and the ground. Positioning the sensor proximal to the ankle joint is ideal to take advantage of the rigid interface between the carbon composite socket and the prosthesis. This location allows a compliant foot structure to be used as an artificial foot to be in contact with the ground. This sensor and its use is described in the following paragraphs.

3.2.6. Force / Torque Transducer

A six axis load cell was selected as an "*observing*" sensing of the forces and torques that interact between the patient and the ground, mounted at proximal to the joint articulation of the prosthetic devices. The load cell is an ATI© six axis force/torque transducer model *Delta* with calibration SI660-60. Commonly used as a wrist sensor for industrial robots, this transducer is a compact, rugged and monolithic structure that converts force and torque into analog strain gauge signals. This sensor is compatible with commercially available general-purpose and high-accuracy data acquisition hardware.
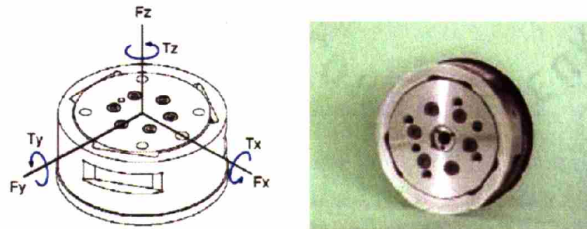
Figure 2-21. ATI Industrial Automation, Inc. force / torque transducer: *Delta*

Fx,Fy	Fz	Tx,Ty	Tz	Fx,Fy	Fz	Tx,Ty	Tz
660 N	1980 N	60 N.m	60 N.m	1/32 N	1/32 N	9/533 N.m	6/533 N.m
	SENSING RANGES				RESOLUTION		

Table 2-2. Load cell model *Delta* standard calibration SI-660-60

42

The load cell was rigidly mounted on passive and active ankle prosthesis between the socket and prosthesis socket adapter. For the passive ankle, the load cell was attached to the pylon and the foot prosthesis, using a standard mounting female prosthetic. For the active ankle, this sensor was installed between the prosthesis and socket with the provided mounting plate and a commercial male to female prosthetic connector. This sensor was an overall weight of 910 g, and is 33.3 mm thick. This dimension allows minimum disturbance in overall length of the prosthetic systems attached to the amputee wearer.
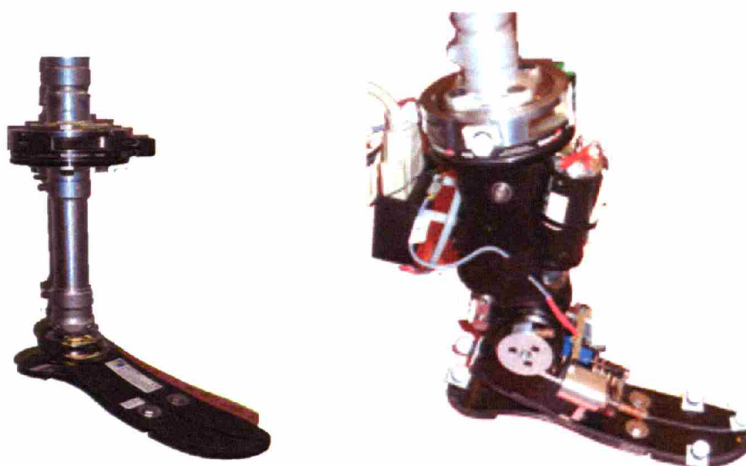
Figure 2-22. Force / torque transducer mounted to passive and active prosthesis.

3.3. Wearable Computing System

The powered ankle-foot used in the experiments was interfaced to a mobile computing platform worn by the user on a hip pack and/or custom backpack. The computing system was in charge of controlling the active-ankle foot prosthesis as well as of monitoring and recording the different sensory information. The signals from the force/torque transducer were recorded separately by another computing system since this transducer was used with two separate prosthetic devices that were tested independently.

In the following sections the different components of the wearable computing system are described.

3.3.1. On-board Computer and Data Acquisition

The onboard computer of the wearable system is a MICROSPACE PC104 Pentium III CPU at 700 MHz (MSMP3XEG) from Advanced Digital Logic, Inc.). This small form factor module CPU with the base boards, integrates all the standard functions of a PC compatible system. It can function under different operating systems and sources (floppy disk, hard disk or compact flash) and has connection to standard computer peripherals.

A multifunctional Input / Output module with a PC104 format,\ from Sensory Co. Inc. (Model526) was interfaced with the PC104 CPU system. This board receives all the information from the sensors and then is processed by the computer on board. The full system runs the Matlab® Kernel for xPC target applications (www.mathworks.com). The onboard computer runs the real-time software and data acquisition routines to control the powered-ankle. The real-time control program is compiled in Matlab® in a host computer and the executable program is then downloaded to the on-board computer's kernel. The communication between the host computer and the on-board system is via TCP/IP. The data is collected and saved in temporal memory of the onboard system and then downloaded to the host computer, once every experimental trial is finalized. The whole mobile platform allows conducting experiments outside a lab setting.
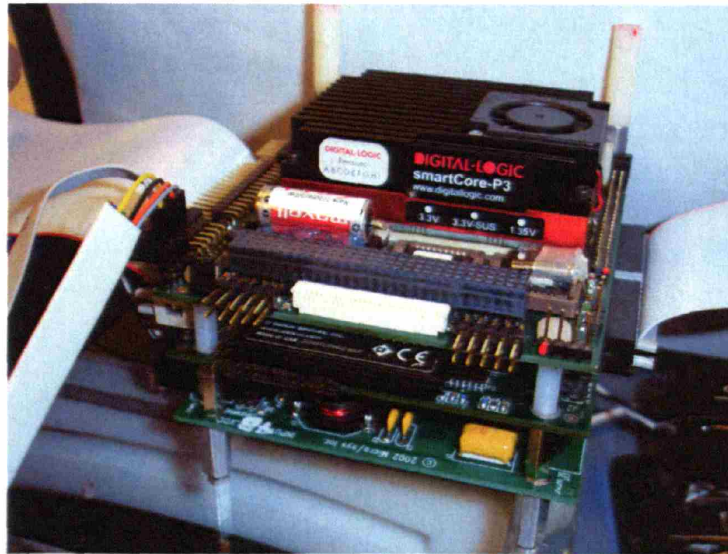
Figure 2-23. On board PC 104 modules

44

3.3.2. Sensory Breakout PCB Boards

Three breakout boards were designed and incorporated into the mobile platform. They interface the information from the variety of sensors mounted on the active ankle with the computing system data acquisition cards. A small breakout board attached to the active ankle concentrates the signals from the sensors in the prosthetic device and transmits them via a DB-25 cable/connector to a second breakout board in the wearable unit that interfaces with the on-board PC104 system. A third general breakout board for the Sensory I/O card was also designed and incorporated to expand the I/O capabilities of the device.
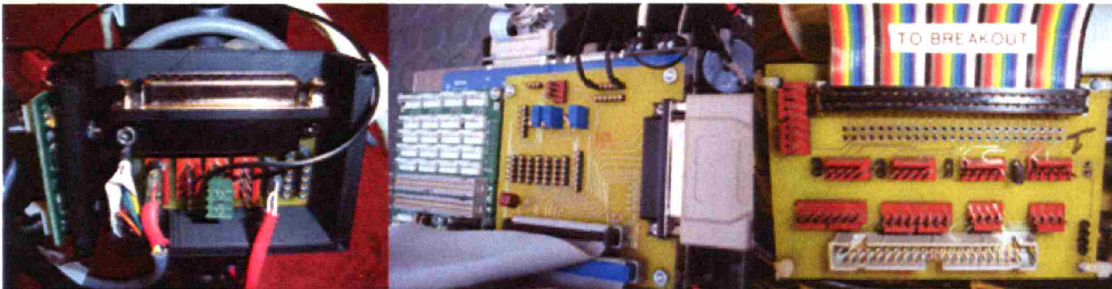
Figure 2-24. Sensory breakout boards.

3.3.3. Power Supply Regulation PCB

The wearable system can be powered via batteries or with a tethered powered supply. In both cases, to provide the required power to the different electronic systems and sensors on wearable computing unit and prostheses, a custom made power supply regulation card was designed. This card can regulate an input of 48V DC 18A, to three output voltages. It regulates +/- 15V 1 A for the ATI force / torque transducer, +/- 12V, 1A for the instrumentation suit (rest of sensors) and +5V, 3A to power the PC104 on-board computer.

Figure 2-25. Power supply regulation PCB.

3.3.4. Actuator Amplifier

A general purpose digital servo amplifier (Accelus ™ ACP-090-36) from Copley Controls Corp. as used to drive the Maxon © DC motor (model RE-max 40®) that powers the active ankle emulator. The amplifier can be used in brushed and brushless modes, offering current, position and velocity controls over the actuators. It can provide 6 Amps of continuous current with peak 36 Amps. This amplifier was chosen based on the maximum continuous current of the DC motor can handle. The interface between the digital amplifier and computing system is done through the general I/O breakout board.

Figure 2-26. Accelus ™ digital amplifier from Copley Controls Corp.

3.3.5. Wearable Computing Pack

In order to hold the electronics in a wearable system, a waist pack was originally designed and tested. This system was made out of nylon composite attached to a military "alise type" belt. The functionality of this device was limited when more electronic components were added. They increased the overall weight of the system making it uncomfortable for the amputee user. An improved version of the system was implemented in a light-weight back/packing frame. This second system has efficiently hold the control electronics and on-board computing system with no discomfort to the user.
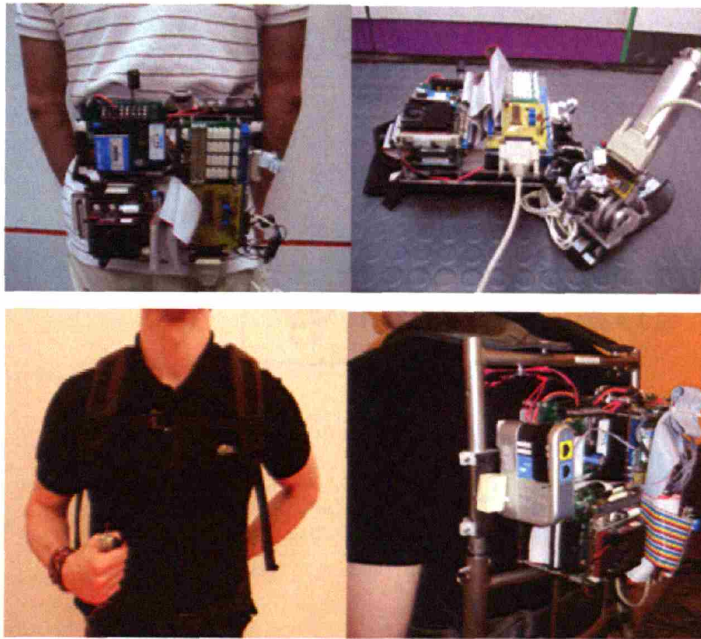
Figure 2-27. a) Original mobile computing platform on waist pack
b) Current wearable back-pack computing system

Power supply regulation   General Break out board

Motor amplifier

Sensory breakout board
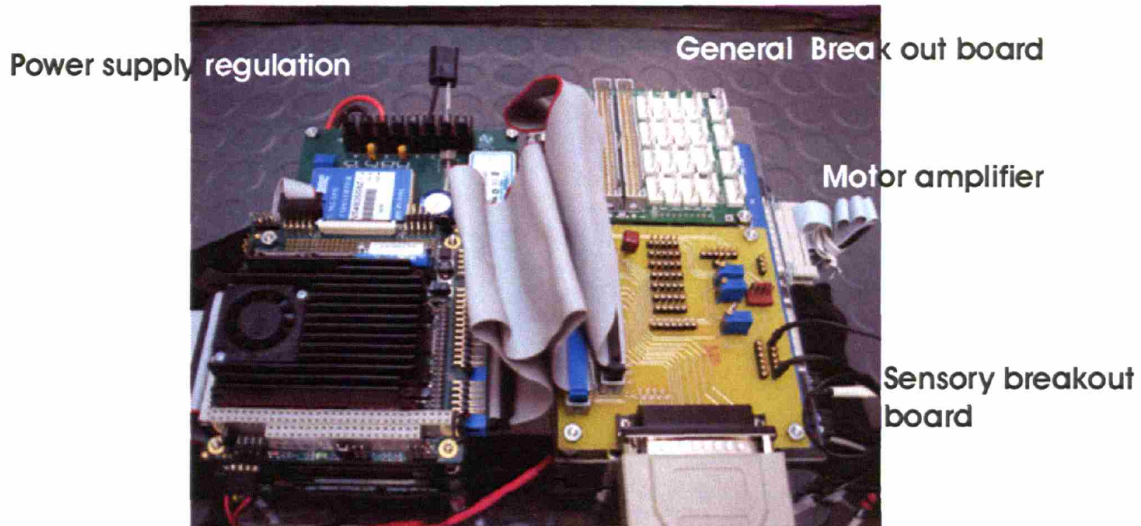
PC104 system with D/A cards

Figure 2-28. Wearable computing system configuration

3.4. Gait Laboratory Instrumentation

The experiments of this investigation were done at MIT' gait laboratory. For this laboratory a new a set of force plates was installed and integrated with a passive, 3D motion capturing system. With this biomechanical analysis tools, the estimation methods of this research were validated.

The 3D Motion system is a Vicon 8®, that consists of 16 infrared cameras that detect the global position of reflective passive markers placed on the subject / device evaluated. The software provided by the company determines the spatial coordinates of each marker in a global frame with a precision of less than 2mm, providing with the necessary kinematic information.

In combination with the motion capture data, a set of two force platforms model BP600900 - 2000 from Advanced Mechanical Technologies, Inc. (AMTI ©), was employed. The plates are capable of precisely measure the ground reaction force and center of pressure location with respect to a local reference frame given by the manufacturers.

4 Experimental Methods

4.1. Experimental Subject

A below-knee amputee subject was recruited to evaluate the estimation methods of ground reaction force and zero moment point on level ground, when using a passive and active-ankle prosthesis. The relevant anthropometric parameters of the subject are presented in the following table.

Subject	Gender	Age (yr)	Mass (Kg)
HH	M	41	70.3

Table 4-1. Participant anthropometric data

The experimental procedures and evaluations of this investigation where similarly tested on a *control weight* lead block of a known mass of 9 Kg attached to each of the prosthetic devices. The *control weight* was used to simplify the estimation methods and calculations, providing a comparison basis to a more complex dynamic human subject.

4.1.1. Human Subject Use Approval

The experiments in this investigation were approved by MIT Committee on the Use of Humans as Experimental Subjects (COUHES). The participant volunteered and was permitted to withdraw from the study at any time.

4.2. Data Collection

The experiments took place at MIT's gait analysis laboratory. In this laboratory the experiments were recorded by several data collection methods:
  a. Wearable computing system and instrumented prosthetic devices
  b. Vicon 3D motion capture system
  c. AMTI Force plate system

The 3D motion capture system and force measuring platforms were used as standard instrumentation tools used in the field of biomechanics to compare the results of the estimation methods employed.

4.2.1. Prosthetic Devices

Both prosthetic devices (passive and active) were instrumented with the force / torque transducer from ATI Automation® installed at the shank level, 12 cm proximal to ankle joint.   This transducer was connected through an interface power supply box to a host desktop PC computer with a 16 bit data acquisition card (National Instruments PCI 6220). The information from this device was recorded at a sampling rate of 1000 Hz. The resolved force / torque information was obtained with acquisition software provided by the manufacturer.

The measured parameters in the active ankle prosthesis are: the ankle angle, ankle torque and temporal contact parameters given by the mounted foot switches. The ankle angle was measured with a digital encoder 500 counts/turn and ankle torque was indirectly measured with a linear potentiometer across the series springs. The signal from these sensors was sampled at 2000Hz.

The signal from the linear potentiometer was conditioned using an analog low pass filter with a cut off frequency of 1.5 KHz. This frequency was adequate to improve signal to noise ratio for the sensor. Temporal parameters sensed by the force sensitive resistors embedded on the sole of the prostheses were sampled at 2000Hz. The force threshold for each sensor was independently selected with a voltage divider according to the subject's weight.

All of the sensors installed in the active ankle-foot emulator where connected to the wearable computing unit via a DB-25 cable/connector.

4.2.2. 3D Motion Capture Data

Kinematic data for the experiments was recorded with a 16 camera motion capture system VICON 810i (Oxford Metrics ®, Oxford, UK) at a frequency of 120Hz. The raw data was processed with VICON Work Station® software. Reflective markers were mounted at nine locations of the ankle-foot prostheses: Two markers were mounted on the hill region, three markers in the forefront of the foot and four markers in the location of the force torque transducer. The spatial resolution of the coordinates for this system is approximately 2 mm. Posterior analysis on marker position was done using mathematical software MATLAB® (MathWorks, Natick, MA).
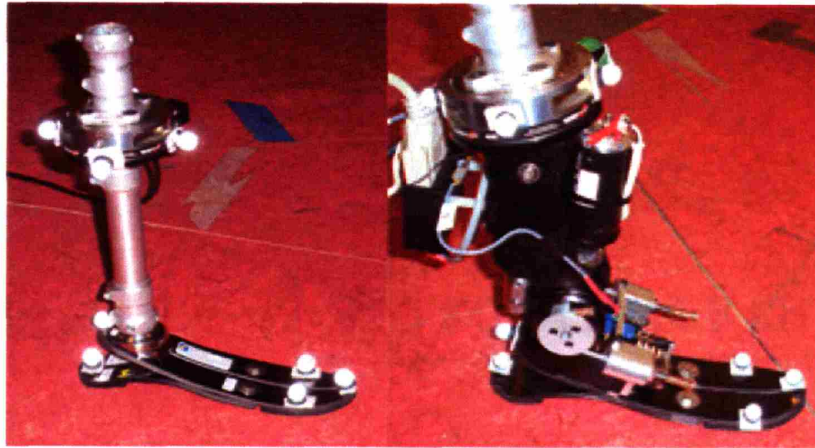
Figure 4-1. Marker location for passive and active ankle prosthesis.

4.2.3. Force Measuring Platforms

During experimental trials an AMTI© force platform system was used to record the ground reaction force. The force data was recorded at a sampling rate of 960Hz at an absolute precision of ~0.1N for vertical ground reaction force and ~2mm for the center of pressure location with respect to the platform's center point. AMTI's ForceNet® and BioAnalysis® analysis programs were used to record and process the experimental data for each trial.

4.3. Experimental Set up
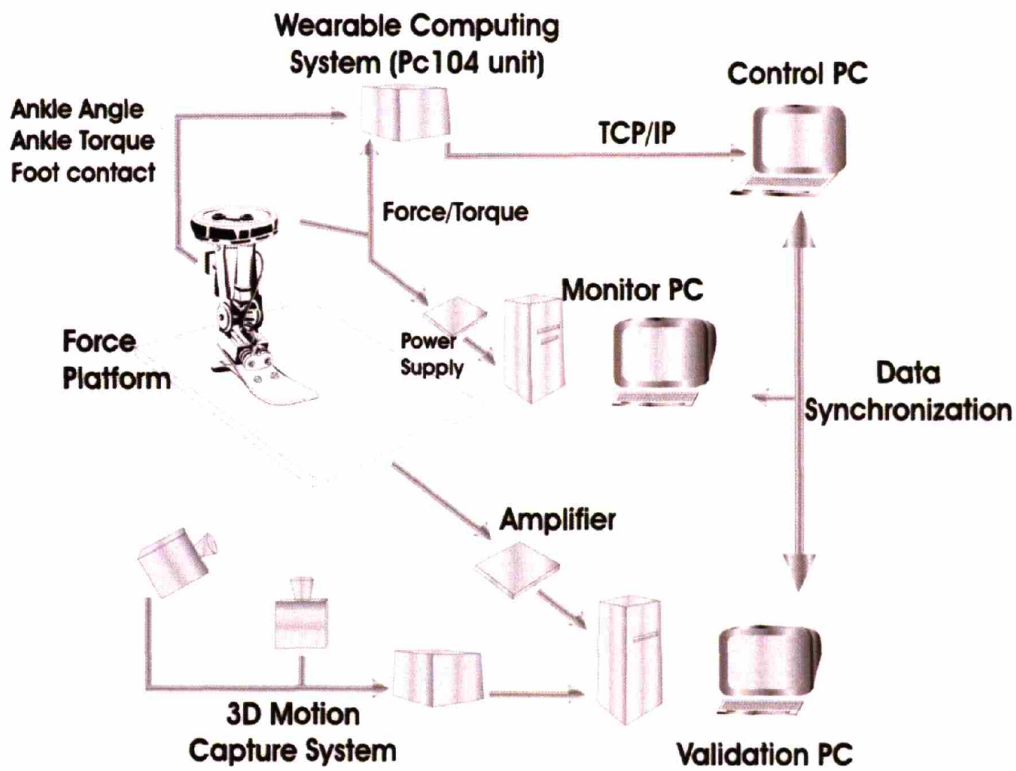
Figure 4-2. Experimental set up. Schematic diagram

The sensory information from the active-ankle prosthesis was sent to the wearable PC104 based computing system where the data was stored in local memory. From there, the data was downloaded to a *Host Control laptop PC*. The values obtained from the force / torque transducer (six-axis load cell) were communicated to a Monitor PC that recorded the sensory information. This torque transducer can also be interfaced directly to the wearable system if desired. In the experiments, this sensor was kept independent from the computing system, deciding to use a *Monitor PC* to record the signals. The reason to keep it independent is that the same series of experiments were performed with an passive device that did not require the use of a wearable computing system.

Simultaneous ground reaction force and kinematic data were recorded with the force plate system and 3D motion capture tool. This information was recorded by a

specific personal computer (*Validation PC*). The signals of the different sensory sources were synchronized at a base frequency of 120 Hz, sampling rate at which the events were recorded by the video capturing system

4.4. Experimental procedure

In this investigation four experimental sessions were performed. Two sessions required the presence of a below-knee amputee and two were performed with a control weight block.

The human subject participated in each of the two experiment sessions in separate days. The first session employed the passive ankle foot prosthesis and the second session incorporated the use of the powered ankle-foot robotic prototype. Each session consisted of three experiments of 10 trials each.

The experiments performed are described in the following paragraphs:

4.4.1. Human Subject.- Single Leg Quiet Stance.

The human subject was asked to stand on his right leg wearing the passive ankle prosthesis with open eyes and asked to stand as still as possible. The participant was allowed to reach and lightly touch a support stool to help maintain his balance. Data was collected for 15 seconds.

On a second session, the experiment was repeated with the active-ankle foot prosthesis. The active ankle-foot emulator was programmed to have a linear stiffness of 6.49 Nm/deg for dorsiflexion (i.e when angle between the shank and the foot's dorso is less than 90 degrees) and a stiffness of 8.32 Nm/deg for plantarflexion (i.e. when angle between the shank and the foot's dorso is greater than 90 degrees). These values allow the ankle joint to have a more natural motion during stance. The stiffness value was selected based on similar values as normal ankle/stiffness during stance (Winter et al., 1998; Loram and Lakie, 2002)

53

4.4.2. Human Subject,- Anterioposterior Sway: Single Leg Support.

In this experiment the subject was asked to stand on his right leg wearing the instrumented prosthesis, with open eyes. While maintaining this position he was asked to shift his center of pressure in the sagittal plane with an oscillatory anterioposterior sway, The participant was allowed to reach and lightly touch a support stool to help maintain his balance. Data was collected for ten trials of fifteen seconds each.

The experiment was performed with both prostheses, passive and active, during two different experimental sessions. When wearing the active-ankle foot emulator the stiffness of the ankle joint was set to 6.49 Nm/deg for dorsiflexion and a stiffness of 8.32 Nm/deg for plantarflexion based on similar values present in humans during single leg stance (Winter et al, 1998; Loram and Lakie; 2002).
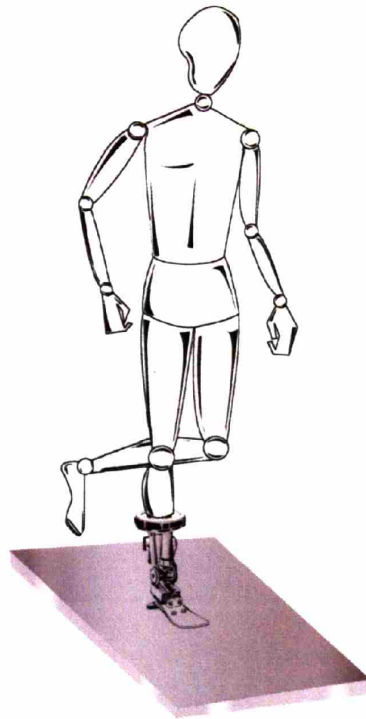
Figure 4-3 Single leg standing experiment

4.4.3. Human Subject.- Slow Walking.

A series of walking experiments were performed with both prosthetic systems. During the assessment, the subject was asked to walk comfortably at a slow speed and make a single step over the force platform. The subject completed some practice walks to ensure that prosthetic foot made adequate contact with the force plate during single support. Ten trials were evaluated for this experiment. When using the active ankle foot emulator, the ankle stiffness was programmed to be same as for the stance experiments. No push off power was provided by the powered ankle-foot prototype to *toe off.*
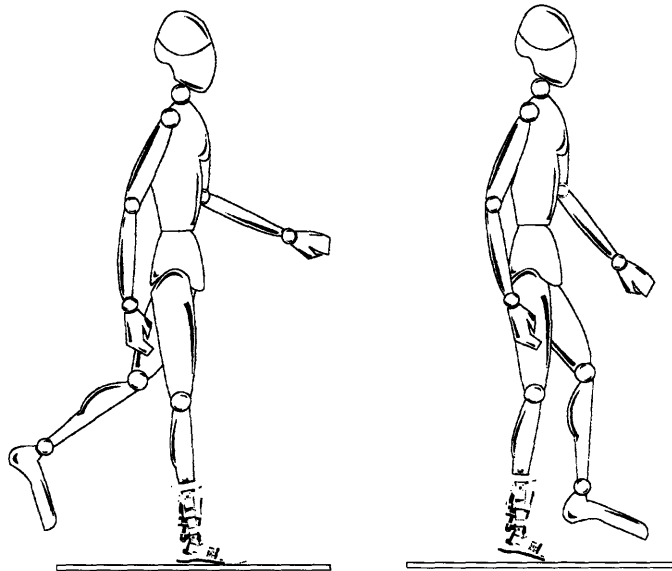
Figure 4-4. Slow walking on force platform

4.4.4. Control Weight . - Stance

Ten trials of thirty seconds each were evaluated using a control weight lead block of 9 Kg during single support stance emulation. In this experiment a control weight block connected to the artificial prostheses (passive and active systems) was kept in a vertical position as still as possible. Light lateral support was provided by hand avoid falling. Stiffness values for the active system were the same as discussed earlier in the human subject experiments.

4.4.5. Control weight. - Anterioposterior Sway

In these series of tests ten trials of thirty seconds each were evaluated with a control weight block attached to the artificial prostheses. The tests consisted in displacing the block with an anterioposterior oscillation to observe the displacement of the center of pressure. In the case of the active system, the value of the stiffness around the ankle joint was programmed to be the same as in the experiments with the human subject.

For all of the experiments described earlier the force platform measured the kinetic data at a frequency of 960 Hz. Three dimension kinematic data, representing the position of the markers attached to the prostheses, was simultaneously recorded at 120Hz. Nine reflective markers were positioned on both artificial ankle-foot devices.

The estimation methods of the ground reaction force and zero moment point location were analyzed and statistically compared, combining the kinetic and kinematic data obtained for each experiment, as described in the following section,

Figure 4-5. Control weight on passive prosthesis with reflective markers and force/torque sensor

4.4.6. Data Processing

Data sets from the different sensory sources were processed and analyzed using Matlab®. Every experimental trial was synchronized and resampled at a rate of 120Hz. Only kinematic information was digitally processed to reduced noise levels inherent of the capturing system.

All kinematic data was low-pass filtered with a zero-phase forward and reverse butterworth digital filter at a cutoff frequency of 20Hz. To remove any phase lag due to the recursive nature of the filter, the information was processed in forward and backward direction. This process helps remove inaccuracies in temporal measurements.

4.5. Data analysis: Static Model

A static model is proposed in order to estimate the ground reaction force vector and location of the zero moment point in the active ankle foot prosthesis and as well as in a commercially passive prosthesis. The estimation contemplates only single stance support (while standing on one leg and during single support in slow walking). The estimated values were compared to the GRF and COP provided by a force platform in conjunction with the kinematic data of the 3D motion capturing system.

The coordinate system employed for the model is Cartesian. The sign convention for the ground reaction force is based on Winter (1987) and Whittle (1991), where the ground reaction force is positive upward and forward.

In the current research four references frames were employed:

a) Reference frame $\{G\}$ - (O_GXYZ) Global reference frame (corresponds to the laboratory's frame established to be the same as the motion capture system's.)

b) Reference frame $\{A\}$ - $(O_AX'Y'Z')$ Force plate reference frame (fixed)

c) Reference frame $\{S\}$ - $(O_SX''Y''Z'')$ - Six axis force / torque sensor frame.

d) Reference frame $\{P\}$ - $(O_PX'''Y'''Z''')$ – center of pressure / zero moment point reference frame (lies within the support polygon formed by the parts of the body in contact with the ground. i.e. prosthetic foot).
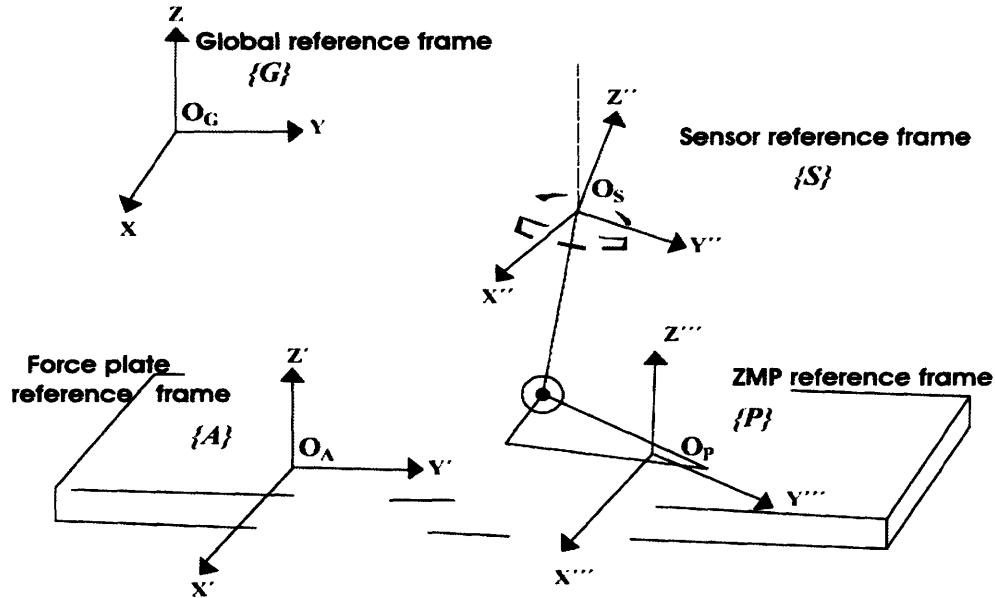
Figure 4-6. Reference frames

The force components interacting with the ground, in particular of the ground reaction force were determined considering both instrumented prosthetic devices as rigid bodies in static equilibrium. With this assumption, we can determine that the summation of forces and moments acting on the devices at any moment in time is zero along and about each of the three Cartesian axes.

$$\sum F = 0 \ ; \sum M = 0$$

The location in space with respect to the global reference frame of the origin O_S (origin of the force/torque transducer mounted of both prosthetic devices) was determined with the help of the four markers mounted on the sensor. These markers defined two orthogonal vectors corresponding to the X" and Y" axes. The average midpoint of the global coordinates of these vectors was considered to be the local sensor origin of frame $\{S\}$. This reference frame has a Z" axis that is coaxial with the long axis of the shank throughout the experiments, while the X" and Y" perpendicular axes represent the mediolateral and anterioposterior direction of the system.

For the active ankle device the kinematic information corresponding to the rotation of the ankle joint was obtained with the digital encoder mounted on the device.

This encoder provides the ankle angle and relative rotation around the parallel *X''* and *Y''* axes of the reference frames *{S}* and *{P}*, attached to the load cell and to the zero moment point, respectively. For the passive ankle no rotation around the ankle joint was assumed.
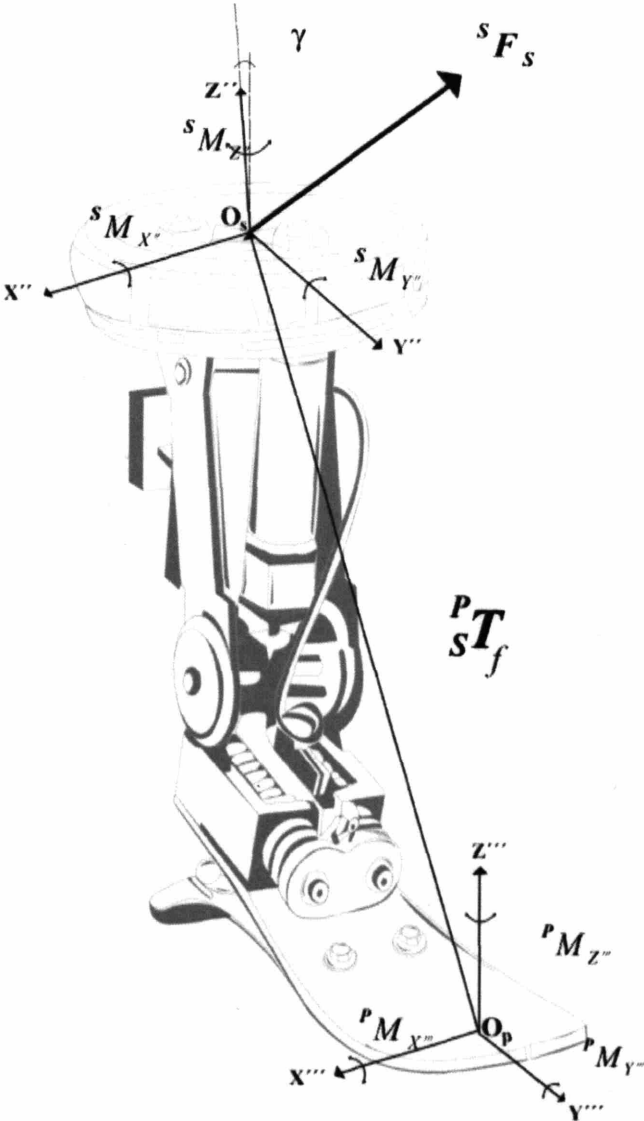
Figure 4-7. Free body diagram for the estimation of the GRF

4.6. Estimation of Ground Reaction Force

A generalized force vector acting on a rigid body can be represented with a 6 x1 matrix:

$$f = \begin{bmatrix} F \\ M \end{bmatrix}$$

Where F is a 3x1 force vector and M is a 3 x 1 moment vector. Considering the instrumented prostheses as rigid bodies the forces that are measured in the $\{S\}$ frame (at the force / torque sensor) can be mapped to the reference frame corresponding to the frame $\{P\}$ at the location of the ZMP (see figure 4-7):

$$^{P}f_{P} = {}^{P}_{S}T_{f}{}^{S}f_{S}$$

Where $^{P}_{S}T_{f}$ is the force-moment transformation matrix of 6 x 6, $^{S}f_{S}$ is the 6x1 vector of the forces and moments measured at the load cell and $^{P}f_{P}$ are the forces and moments interacting with the ground at the zero moment point, with respect to frame $\{P\}$.

This transformation can be described as:

$$\begin{bmatrix} ^{P}F_{P} \\ ^{P}M_{P} \end{bmatrix} = \begin{bmatrix} ^{P}_{S}R & 0 \\ \vec{r}_{PS} \times {}^{P}_{S}R & {}^{P}_{S}R \end{bmatrix} \begin{bmatrix} ^{S}F_{S} \\ ^{S}M_{S} \end{bmatrix}$$

Where $^{P}_{S}R$ and $\vec{r}_{PS}$ are rotation and translation matrices respectively, that relate frames $\{S\}$ relative to $\{P\}$.

If the only mapping of interest is the force vector, the following part of the transformation is considered:

$$\left[^{P}F_{P}\right]=\left[^{P}_{S}R\right]\left[^{S}F_{S}\right]$$

For this transformation it is assumed that adduction-abduction of the foot-ankle is negligible and that the {S} and {P} frames are coplanar, rotated with an angle of γ around the X''' axis

$$^{P}_{S}R=\begin{bmatrix} 1 & 0 & 0 \\ 0 & \cos\gamma & -\sin\gamma \\ 0 & \sin\gamma & \cos\gamma \end{bmatrix}$$

The forces that interact with the ground, relative to frame {P}, can then be expressed as:

$$^{P}F_{x''}={}^{S}F_{x''}$$
$$^{P}F_{y''}={}^{S}F_{y''}\cos\gamma-{}^{S}F_{z''}\sin\gamma$$
$$^{P}F_{z''}={}^{S}F_{y''}\sin\gamma+{}^{S}F_{z''}\cos\gamma$$

Here the left superscript represents the reference frame and the right subscript represents the co-ordinate direction. These mappings should be interpreted as instantaneous results because the ZMP is constantly moving and the relationship between both reference frames is not static.

In order to compare these estimations with the measured ground reaction forces by the force platform a new transform has to be made. The estimated forces represented relative to frame {P} should be represented relative to frame {A} (force plate reference frame). The kinematic information to reference both systems is obtained using the 3D motion capture data. The transformation is:

$$\left[^{A}F_{A}\right]=\left[^{A}_{P}R\right]\left[^{P}F_{P}\right]$$

Where is the rotation matrix relating both frames is:

$$
{}^A_P R = \begin{bmatrix} \hat{x}_P \cdot \hat{x}_A & \hat{y}_P \cdot \hat{x}_A & 0 \\ \hat{x}_P \cdot \hat{y}_A & \hat{y}_P \cdot \hat{y}_A & 0 \\ 0 & 0 & 1 \end{bmatrix}
$$

This matrix is composed of the dot product of the pair of unit vectors that define both horizontal axes. Both frames are at ground level and are coplanar. The angle α is the rotation around the Z' axis of frame {A}.

The resulting force representation of the components of the GRF measured in the sensor frame {S} relative to frame {A} are:

$$
{}^A F_{x'} = {}^S F_{x''} \cdot \cos\alpha + {}^S F_{y''} \cdot \cos\gamma \sin\alpha - {}^S F_{z''} \sin\gamma\sin\alpha
$$
$$
{}^A F_{y'} = -{}^S F_{x''} \cdot \sin\alpha + {}^S F_{y''} \cdot \cos\gamma\cos\alpha - {}^S F_{z''} \sin\gamma\cos\alpha
$$
$$
{}^A F_{z'} = {}^S F_{y''} \sin\gamma + {}^S F_{z''} \cos\gamma
$$

4.7. Estimation of Zero Moment Point
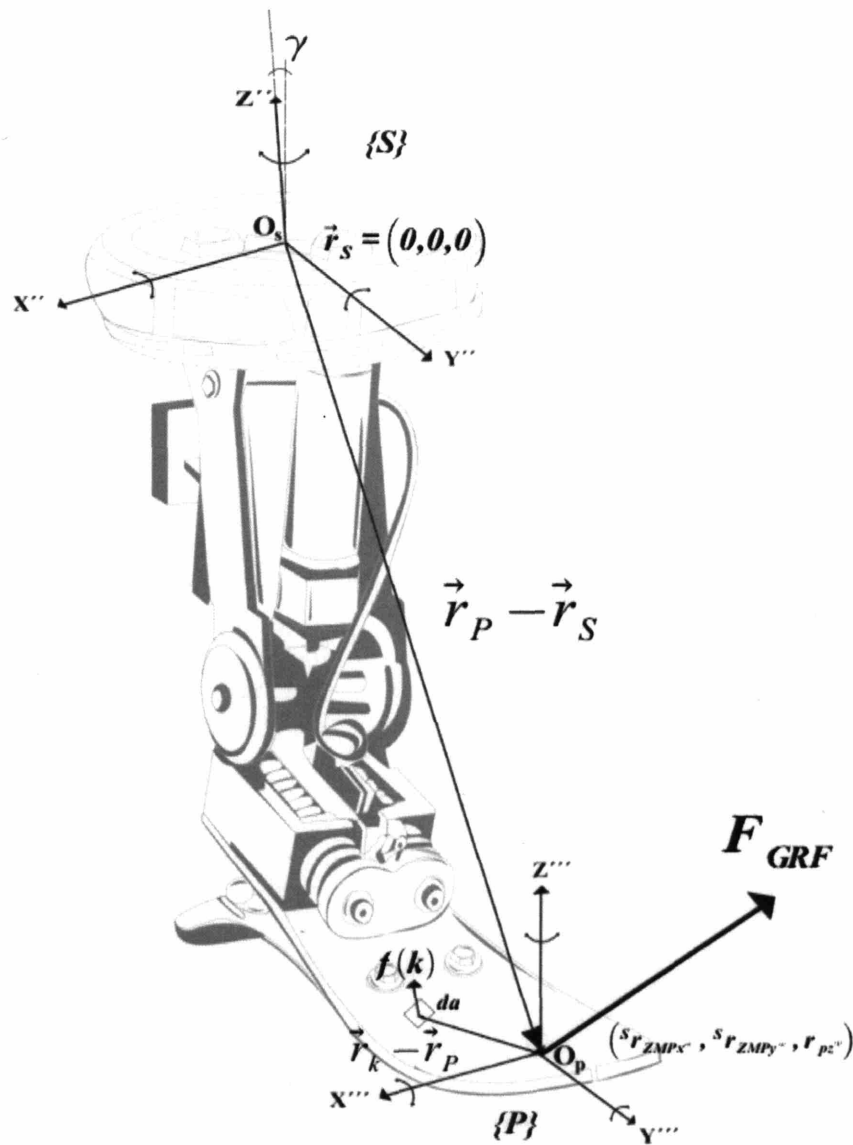
Figure 4-8. Free body diagram of foot/ankle complex for determination of ZMP

Figure 4-8 represents the free body diagram of the foot ankle complex analyzed to determine the location of the ZMP. For this analysis, the foot/ankle complex was considered a rigid body in static equilibrium. The area of the foot in contact with the ground surface is referred to as the ground support base (*g.s.b.*) and the only external

force acting on it is the ground reaction force. Assuming that the only area in contact with the ground is the g.s.b, it can be considered the support polygon.

Defining the moments induced the ground reaction force at O_P and at O_S.

At O_P:

$$M_P = \int_{gsb} \left(\vec{r}_k - \vec{r}_P \right) \times f(k) \, da$$

where

M_P = Moment around system $\{P\}$ whose origin is O_P

$\vec{r}_k$ is the location of a point k in the ground support base (g.s.b.) ;

$\vec{r}_P$ is the vector that defines the position of the zero moment point at O_P;

$f(k)$ is the force acting on the point k

da is an infinitesimal element of the support surface.

At O_S the moment can be defined as :

$$M_S = \int_{gsb} \left(\vec{r}_k - \vec{r}_S \right) \times f(k) \, da$$

Where $\vec{r}_S$ is the vector that defines the location of O_S and $\vec{r}_K - \vec{r}_S$ is the vector that goes from the point of application of the force $f(k)$ to this point .

64

This moment can also be expressed as:

$$M_S = \int_{gsb} \left\{ \left(\vec{r}_k - \vec{r}_P\right) + \left(\vec{r}_P - \vec{r}_S\right) \times f(k) \right\} da:$$

$$= \int_{gsb} \left(\vec{r}_k - \vec{r}_P\right) \times f(k)\, da + \int_{gsb} \left(\vec{r}_P - \vec{r}_S\right) \times f(k)\, da$$

$$= M_P + \left(\vec{r}_P - \vec{r}_S\right) \times \int_{gsb} f(k)\, da \;;$$

Where $\displaystyle\int_{gsb} f(k)\, da = F_{GRF}$ is the integration of all ground reaction force vector applied at

the zero moment point (center of pressure).

From the static equilibrium assumption the moment at system {S} is:

$$M_S = M_P + \left(\vec{r}_P - \vec{r}_S\right) \times F_{GRF} \quad (1)$$

considering the cross product we have that:

$$\left(\vec{r}_P - \vec{r}_S\right) \times F_{GRF} = \begin{vmatrix} \hat{i}_S & \hat{j}_S & \hat{k}_S \\ r_{px} - r_{sx} & r_{py} - r_{sy} & r_{pz} - r_{sz} \\ {}^{S}F_{x''} & {}^{S}F_{y''} & {}^{S}F_{z''} \end{vmatrix}$$

If the origin for this analysis is at O_S then :

$$\vec{r}_S = \begin{bmatrix} r_{sx''} & r_{sy''} & r_{sz''} \end{bmatrix} = [0\,0\,0];$$

and the cross product is then:

$$\left(\vec{r}_P - \vec{r}_S\right) \times F_{GRF} = \begin{vmatrix} \hat{i}_S & \hat{j}_S & \hat{k}_S \\ r_{px''} & r_{py''} & r_{pz''} \\ {}^{S}F_{x''} & {}^{S}F_{y''} & {}^{S}F_{z''} \end{vmatrix}$$

According to its definition, at the zero moment point, the torque around the horizontal axes is zero:

$$M_P = \begin{bmatrix} 0 & 0 & {}^P M_{z''} \end{bmatrix}^T$$

Based on the components of M_S we then determine the vector $\vec{r}_P = \begin{bmatrix} r_{px''} & r_{py''} & r_{pz''} \end{bmatrix}$ which is the location of the zero moment point in relation to the {S} reference frame :

$$^S r_{ZMPx''} = r_{px''} = \frac{-{}^S M_{y''} - \left(r_{pz''} \cdot {}^S F_{x''} \right)}{{}^S F_{z''}}$$

$$^S r_{ZMPy''} = r_{py''} = \frac{{}^S M_{x''} - \left(r_{pz''} \cdot {}^S F_{y''} \right)}{{}^S F_{z''}}$$

Where

$^S M_{y''}$, $^S F_{y''}$ - Moment and force, respectively around the Y'' axis of frame {S}

$^S M_{x''}$, $^S F_{x''}$ - Moment and force, respectively around the X'' axis of frame {S}

$^S F_{z''}$ - Force in the Z'' direction of frame {S}.

$r_{pz''}$ - Distance in Z'' to the zero moment point, which for the case of the passive ankle foot prosthesis is a fixed value of -200 mm, since the system does not have an articulated joint. For the active system this value was considered to be -200 cosγ. asumming only rotation in the sagittal plane with no adduction-abduction in the joint.

The estimated ZMP relative to the frame *{S}* and the values calculated with the instruments of the gait lab relative to frame *{P}* were compared in the global coordinate frame *{G}*. The transformations that related the global reference frame *{G}* to the reference frame of foot/ankle force sensor *{S}* and of the force plates *{A}* are:

$$
{}^{G}C = {}^{G}_{S}T \; {}^{S}C = \begin{bmatrix} ZMP_x \\ ZMP_y \\ 0 \\ 1 \end{bmatrix} = \begin{bmatrix} \hat{X}_S \cdot \hat{X}_G & \hat{Y}_S \cdot \hat{X}_G & \hat{Z}_S \cdot \hat{X}_G & r_{sx} \\ \hat{X}_S \cdot \hat{Y}_G & \hat{Y}_S \cdot \hat{Y}_G & \hat{Z}_S \cdot \hat{Y}_G & r_{sy} \\ \hat{X}_S \cdot \hat{Z}_G & \hat{Y}_S \cdot \hat{Z}_G & \hat{Z}_S \cdot \hat{Z}_G & r_{sz} \\ 0 & 0 & 0 & 1 \end{bmatrix} \begin{bmatrix} r_{px''} \\ r_{py''} \\ r_{pz''} \\ 1 \end{bmatrix}
$$

$$
{}^{G}D = {}^{G}_{A}T \; {}^{A}D = \begin{bmatrix} COP_x \\ COP_y \\ 0 \\ 1 \end{bmatrix} = \begin{bmatrix} \hat{X}_A \cdot \hat{X}_G & \hat{Y}_A \cdot \hat{X}_G & \hat{Z}_A \cdot \hat{X}_G & r_{ax} \\ \hat{X}_A \cdot \hat{Y}_G & \hat{Y}_A \cdot \hat{Y}_G & \hat{Z}_A \cdot \hat{Y}_G & r_{ay} \\ \hat{X}_A \cdot \hat{Z}_G & \hat{Y}_A \cdot \hat{Z}_G & \hat{Z}_A \cdot \hat{Z}_G & r_{az} \\ 0 & 0 & 0 & 1 \end{bmatrix} \begin{bmatrix} r_{ax'} \\ r_{ay'} \\ r_{az'} \\ 1 \end{bmatrix}
$$

Here C represents the estimated ZMP values matrix and D the measured COP data from the force plates and T the homogenous transformation to go from one reference frame to the other.

$\begin{bmatrix} r_{px''} & r_{py''} & r_{pz''} \end{bmatrix}^{T}$ represent the location of the ZMP with relative to frame *{S}*

$\begin{bmatrix} r_{ax'} & r_{ay'} & r_{az'} \end{bmatrix}^{T}$ represent the location of the ZMP relative to frame *{A}*

$\begin{bmatrix} ZMP_x & ZMP_y & 0 \end{bmatrix}^{T}$ represent the location of the ZMP in the global frame *{G}*

$\begin{bmatrix} COP_x & COP_y & 0 \end{bmatrix}^{T}$ represent the location of the ZMP given by the force plates in the global frame *{G}*

For level ground walking the ZMP and the COP are the same point. In this investigation the estimated ZMP is compared to the ZMP provided by the force plate measurements and motion capture data. The components of the latter vector were named COP_X, COP_Y just as an aid to distinguish between the estimated and measured ZMP locations.
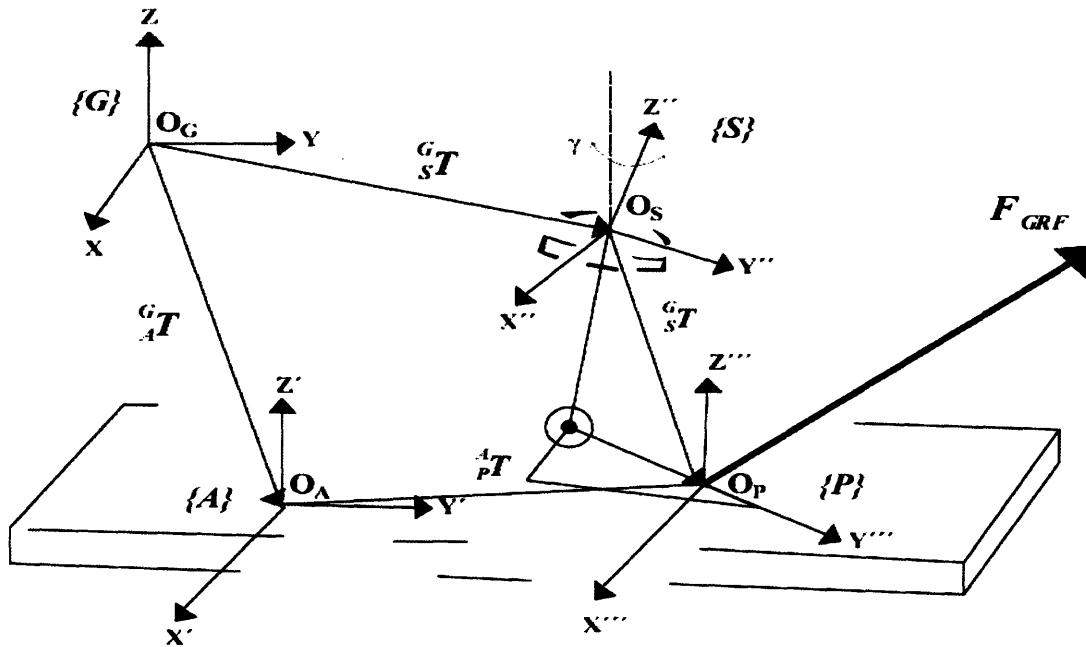
Figure 4-9. Transformations between reference frames

4.8. Statistical Analysis

The root mean square error (RMS error) and the correlation coefficient (R) were computed between the GRF, measured with the force plates, and the estimated values using the sensors the ankle foot prosthesis. The same parameters were calculated to compare the components of the ZMP of the estimated and measured values. The ZMP components were compared relative to the global coordinate frame {G}. These statistical parameters were calculated for each one of the trials of the experiments with the human subject wearing the active and passive prosthesis and with the control weight block.

5 Results

For each one of the experimental trials the root mean square error (RMS error) and the correlation coefficient (R) were calculated. These metrics compare the estimated parameters and the measured values of the ground reaction force components and the ZMP location. The GRF components are compared in the force plate reference frame *{A}*. The vertical component of the force is FZ, the fore-aft component is FY and the medio-lateral component is FX. The ZMP is compared relative to the global reference frame *{G}*.

For the single leg support experiments only ten seconds of data during steady state of the trials are analyzed and presented. During the walking experiments the data analyzed was only during single leg support.

In the following section, a table for each experiment presents the results of the difference for the GRF components and the ZMP. These results are the average and standard deviation of the RMS error as well as the average correlation coefficient. After each table, a particular trial for the experiment of every session is represented graphically. In this representation, the estimated and measured GRF components and the ZMP trajectories are compared. The estimated values were obtained using a static model in combination with the information of the sensorial data coming from the instrumented prostheses and wearable computing system. The validation measurements were obtained from kinetic and kinematic data of a calibrated force platform and reflective motion capture system. In summary, using a static analysis procedure, the estimation of the vertical component of GRF had an averaged correlation coefficient higher than 0.96. The estimated ZMP location had a distance error of less than 1 cm, equal to 4% of the anterior-posterior foot length or 12% of the medio-lateral foot width.

5.1. Human Subject.- Single Leg Quiet Stance. Passive Ankle-Foot

Parameter	RMS ERROR (N)		R
	MEAN	STDV	
FZ	0.3498	0.0684	0.9887
FY	2.5119	0.8586	0.2336
FX	2.2359	0.6010	0.2595

Parameter	RMS ERROR (mm)		R
	MEAN	STDV	
ZMP Y	1.1308	0.3520	0.9043
ZMP X	1.1308	0.3391	0.9197

Average distance between estimated and measured ZMP location : 1.3495 mm

Table 5-1 Experimental results. Human subject single leg quiet stance. Passive ankle-foot
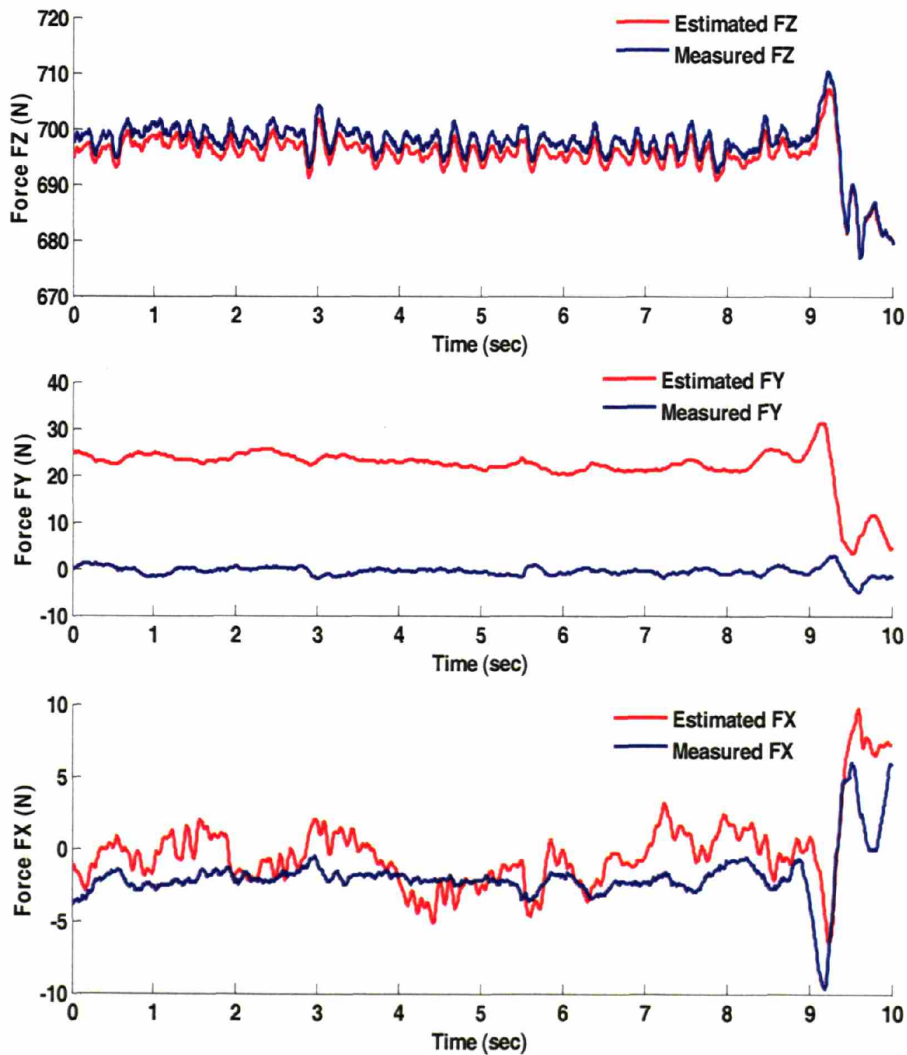
Figure 5-1 Estimated and measured GRF components, relative to force plate reference frame {A} for a single trial. Subject in single support quiet stance with passive ankle-foot

a)
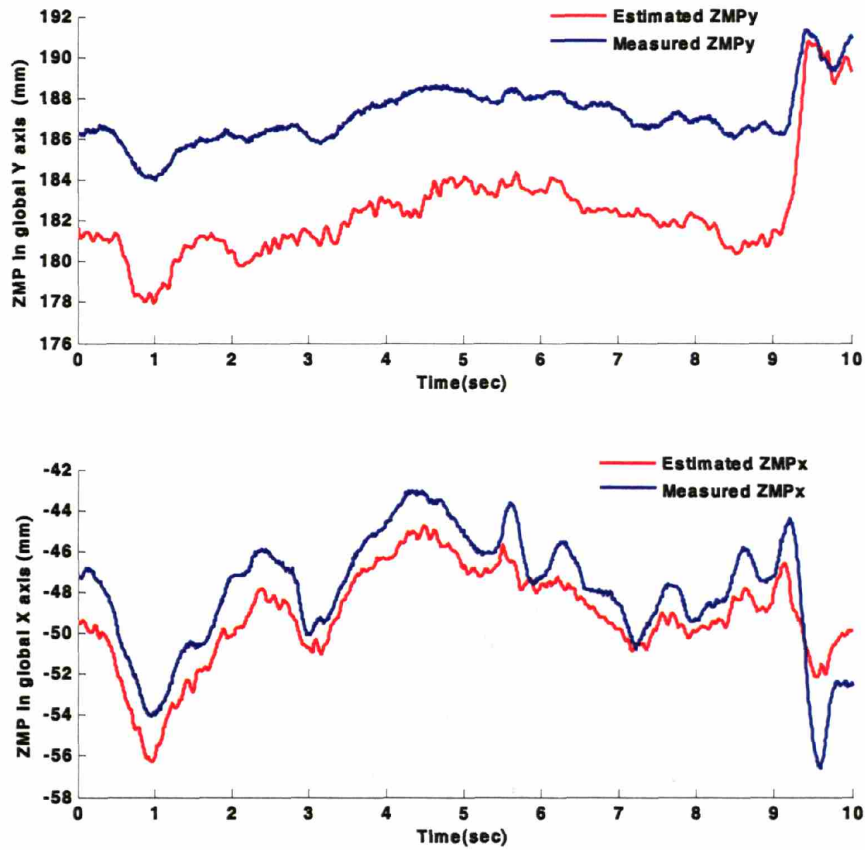
b)
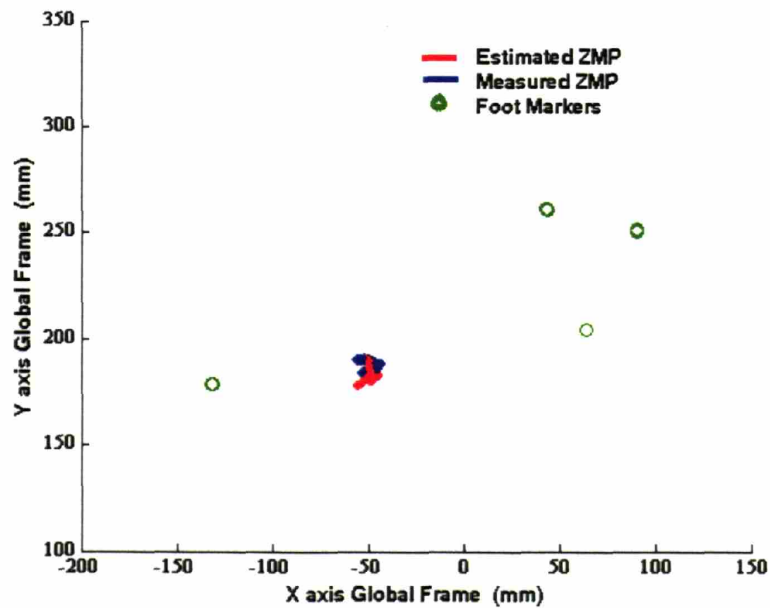
Figure 5-2 a)ZMP trajectory relative to the X and Y axis of the global coordinate frame *{G}* for a single trial. Human subject single support, quiet stance, with passive ankle-foot prosthesis.
b) ZMP trajectory in horizontal plane and its relation with the foot support polygon delimited by the reflective markers of the foot.

71

5.2. Human subject.- Anterioposterior Sway, Single Leg Support. Passive Ankle-Foot

Parameter	RMS ERROR (N)		R
	MEAN	STDV	
FZ	1.569	0.2045	0.9903
FY	7.4534	1.2293	0.7229
FX	15.017	1.6058	0.3511

Parameter	RMS ERROR (mm)		R
	MEAN	STDV	
ZMP Y	4.36	0.8209	0.9897
ZMP X	5.28	1.0772	0.9955

Average distance between estimated and measured ZMP location: 6.102 mm

Table 5-2. Experimental results. Human subject, anterioposterior sway. Passive ankle-foot
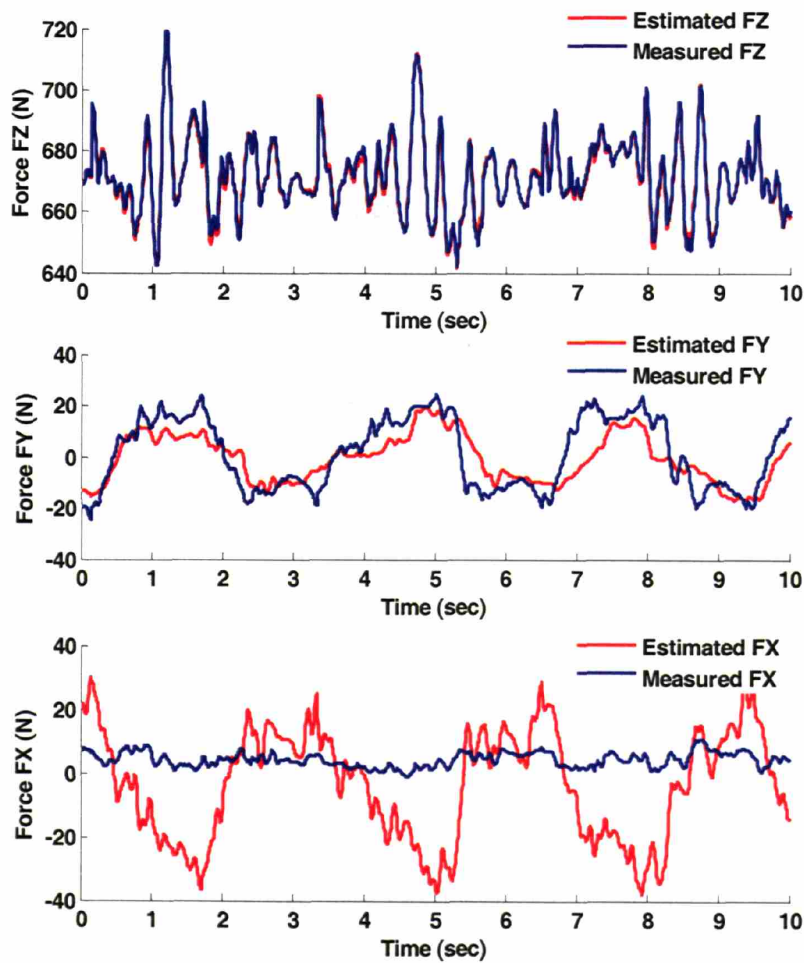
Figure 5-3. Estimated and measured GRF components, relative to force plate reference frame *{A}* for a single trial. Anterioposterior sway single support with passive ankle-foot.

a)
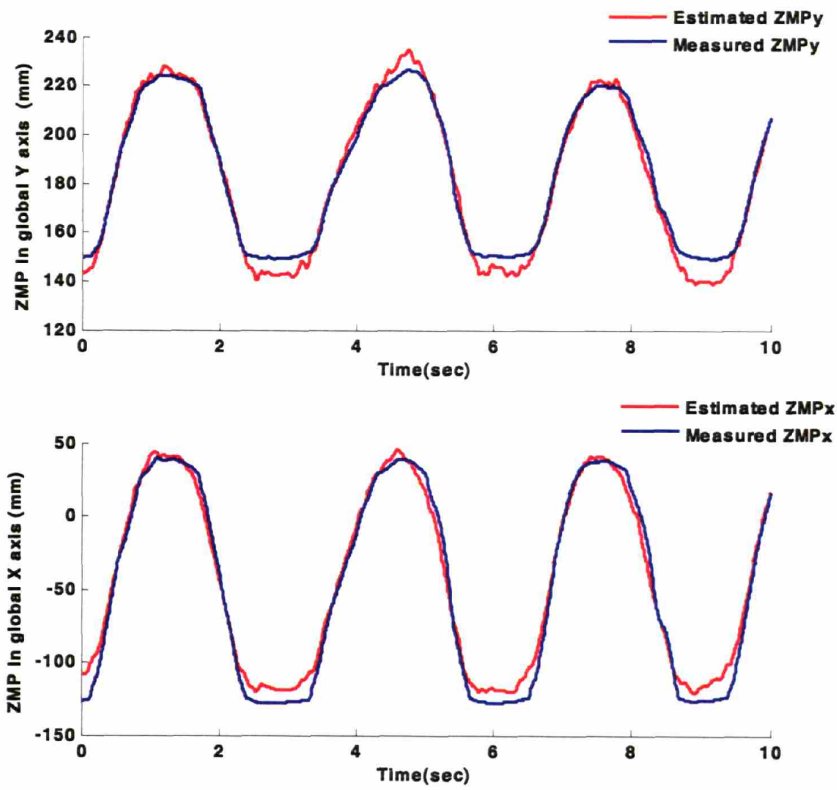
b)
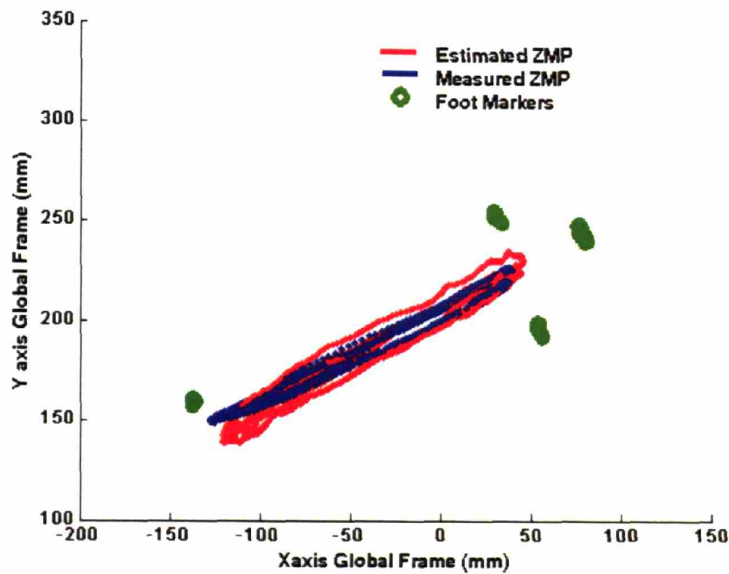
Figure 5-4. a)ZMP trajectory relative to the X and Y axis of the global coordinate frame *{G}* for a single trial b) ZMP trajectory its relation with the foot support polygon delimited by the reflective markers. Anterioposterior sway in single support with passive ankle-foot.

73

5.3.   Human Subject. – Slow Walking. Single Leg Support

Parameter	RMS ERROR (N)		R
	MEAN	STDV	
FZ	3.5451	0.5454	0.9984
FY	4.4954	1.7912	0.5416
FX	13.399	2.8315	0.4671

Parameter	RMS ERROR (mm)		R
	MEAN	STDV	
ZMP Y	5.4388	1.3853	0.9504
ZMP X	9.0299	1.6693	0.9859

Average distance between estimated and measured ZMP location: 9.0119 mm

Table 5-3. Experimental results. Human subject slow walking, single leg support
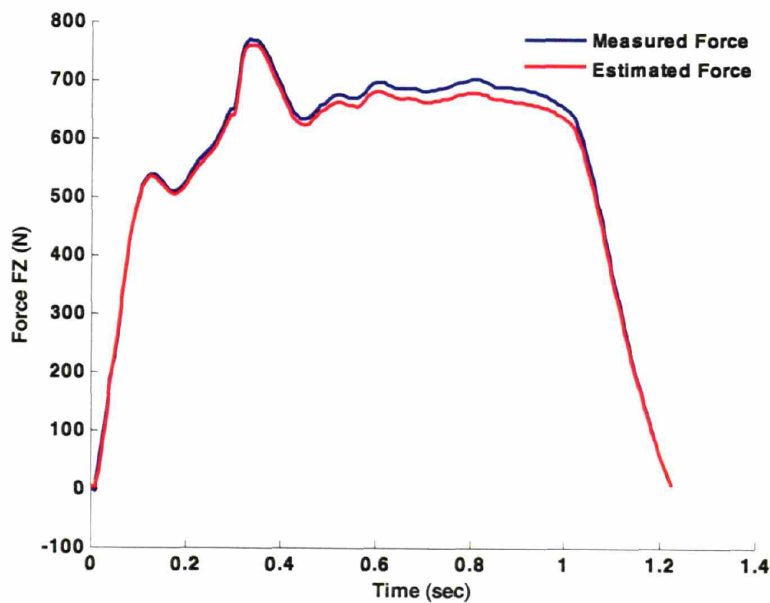
Figure 5-5. Vertical GRF component FZ from hill strike to toe off. Human subject with passive ankle-foot prosthesis.

74
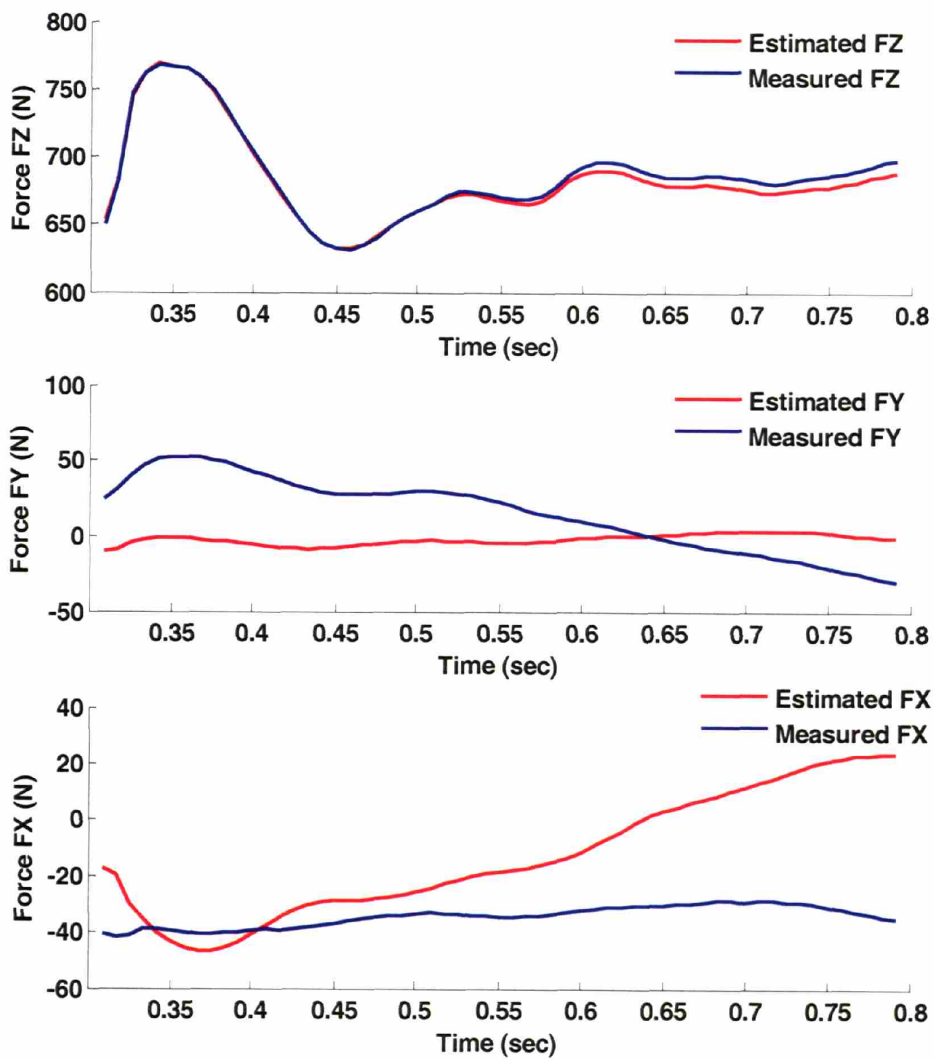
Figure 5-6. Estimated and measured GRF components relative to reference frame *{A}* single leg support during slow walking trial. Human subject with passive-ankle prosthesis.

a)
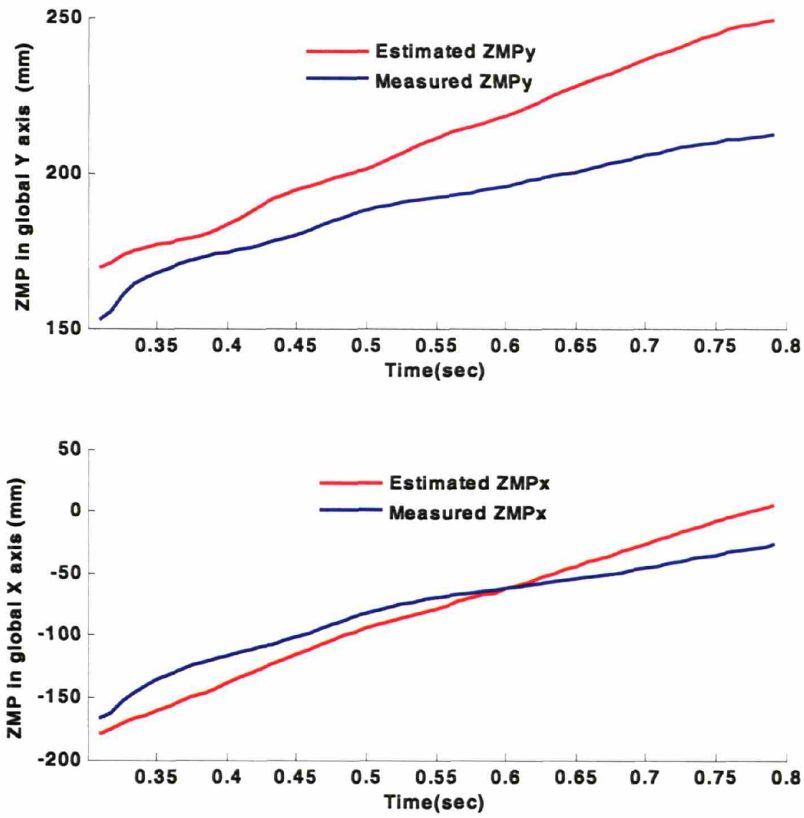
b)
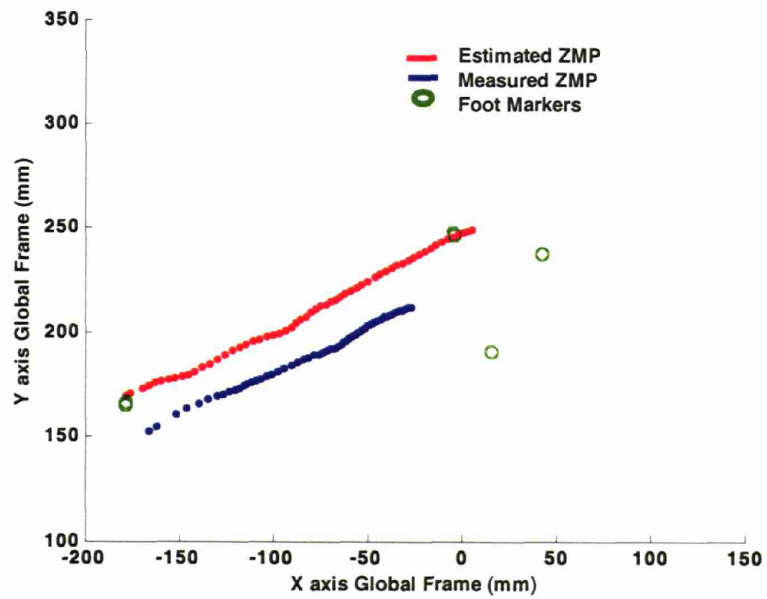
Figure 5-7. a) ZMP trajectory relative to the X and Y axis of the global coordinate frame {G} during single leg support in slow walking with passive ankle-foot. b) ZMP trajectory in global coordinates for single trial and its relation with the foot support polygon delimited by the reflective markers.

5.4. Human Subject.- Single Leg Quiet Stance. Active Ankle-Foot

Parameter	RMS ERROR (N)		R
	MEAN	STDV	
FZ	1.9350	0.7685	0.8303
FY	3.3451	0.6587	0.1870
FX	7.1954	6.7288	0.2764
Parameter	RMS ERROR (mm)		R
	MEAN	STDV	
ZMP Y	1.6647	0.3191	0.8677
ZMP X	1.6874	0.1425	0.8341

Average distance between estimated and measured ZMP location : 2.148 mm

Table 5-4. Experimental results. Human subject single leg quiet stance. Active ankle-foot
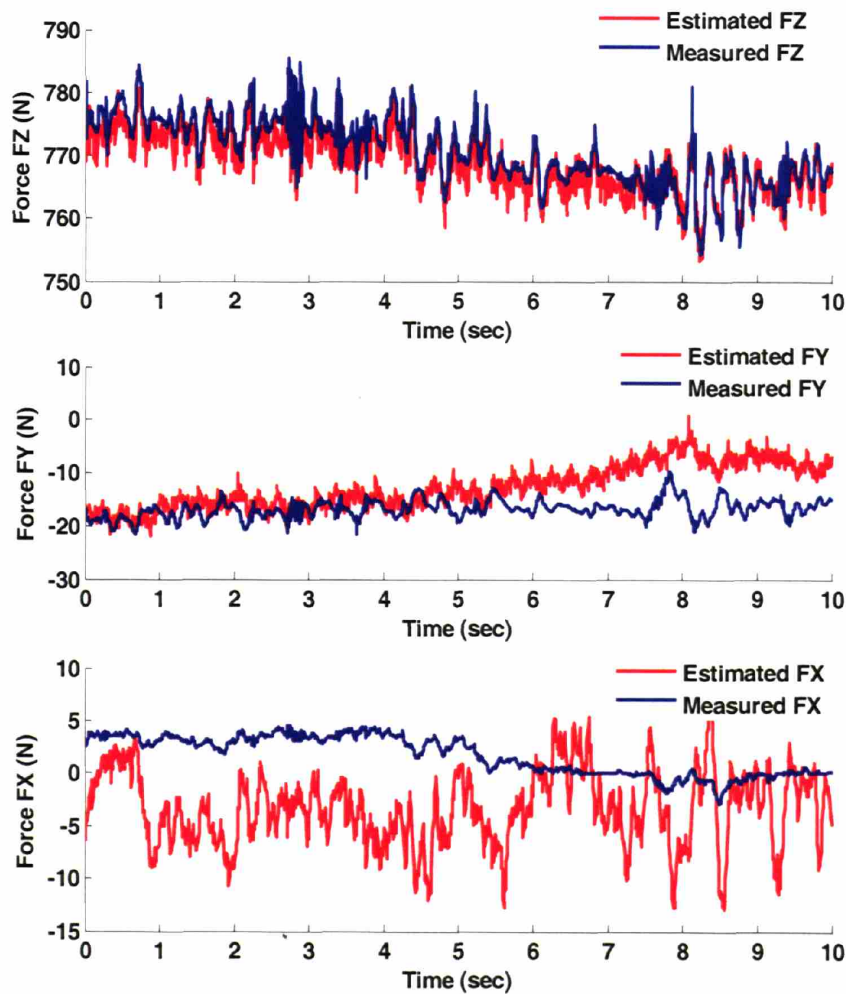
Figure 5-8. Estimated and measured GRF components, quiet standing single leg support during one trial, in reference to frame {A}. Human subject with active ankle-foot prosthesis.

77

a)
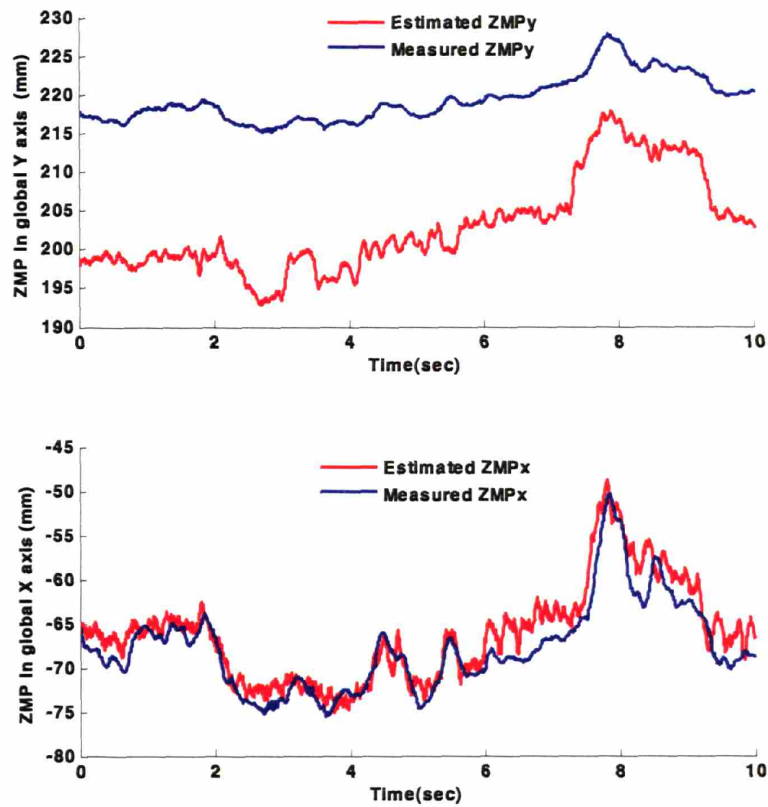
b)

Figure 5-9. a)ZMP trajectory relative to the X and Y axis of the global coordinate frame *{G}* during single support quiet stance with active ankle-foot) ZMP trajectory in global coordinate frame and its relation with the foot support polygon delimited by the reflective markers.

5.5. Human subject.- Anterioposterior Sway, Single Support. Active Ankle-Foot

Parameter	RMS ERROR (N)		R
	MEAN	STDV	
FZ	12.344	9.5536	0.9678
FY	4.5049	0.8585	0.4489
FX	7.2447	1.2435	0.3851
Parameter	RMS ERROR (mm)		R
	MEAN	STDV	
ZMP Y	2.5798	0.5353	0.9737
ZMP X	3.2589	0.4476	0.9901

Average distance between estimated and measured ZMP location : 3.674 mm

Table 5-5. Experimental results. Human subject anterioposterior sway. Active ankle-foot

Figure 5-10. Estimated and measured GRF components relative to frame {A}. Anterioposterior sway during single leg support. Human subject with active ankle prosthesis, single trial.

a)

b)
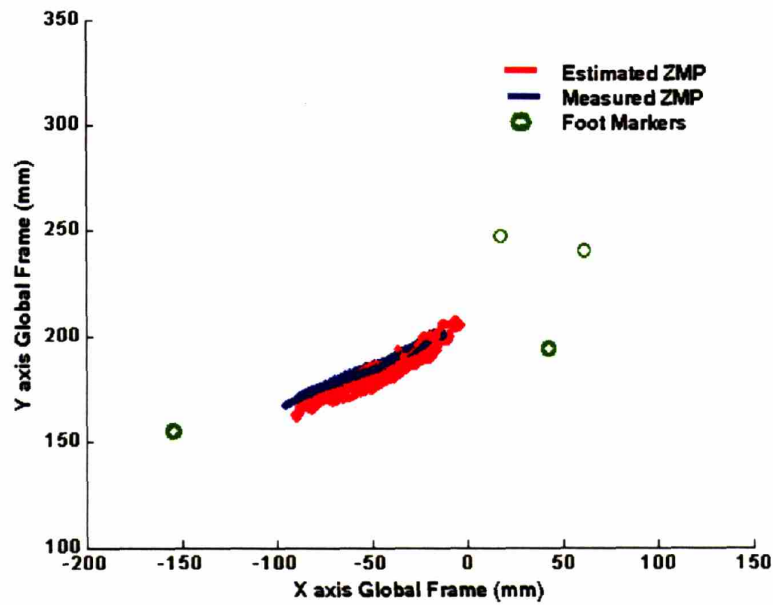
Figure 5-11. a)ZMP trajectory relative to the X and Y axis of the global coordinate frame {G} during anterioposterior sway while standing on single leg with active ankle-foot b) ZMP trajectory in global coordinate frame and its relation with the foot support polygon delimited by the reflective markers.

5.6.   Control Weight. - Stance. Passive Ankle-Foot

Parameter	RMS ERROR (N)		R
	MEAN	STDV	
FZ	0.2464	0.0273	0.8057
FY	0.4171	0.1565	0.4078
FX	0.3227	0.1324	0.3219

Parameter	RMS ERROR (mm)		R
	MEAN	STDV	
ZMP Y	0.9751	0.4588	0.9575
ZMP X	2.5888	0.8631	0.3748

Average distance between estimated and measured ZMP location : 2.507 mm

Table 5-6. Experimental results. Control weight stance. Passive ankle-foot
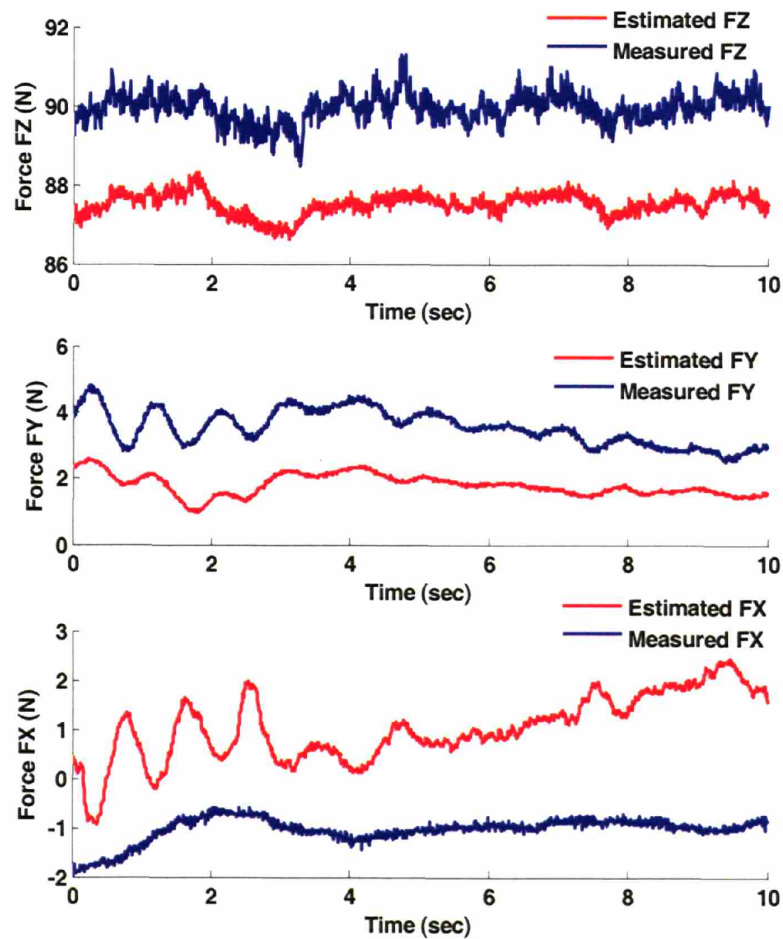
Figure 5-12. Estimated and measured GRF components relative to frame *{A}*, quiet stance with control weight and passive ankle-foot prosthesis. Single trial.
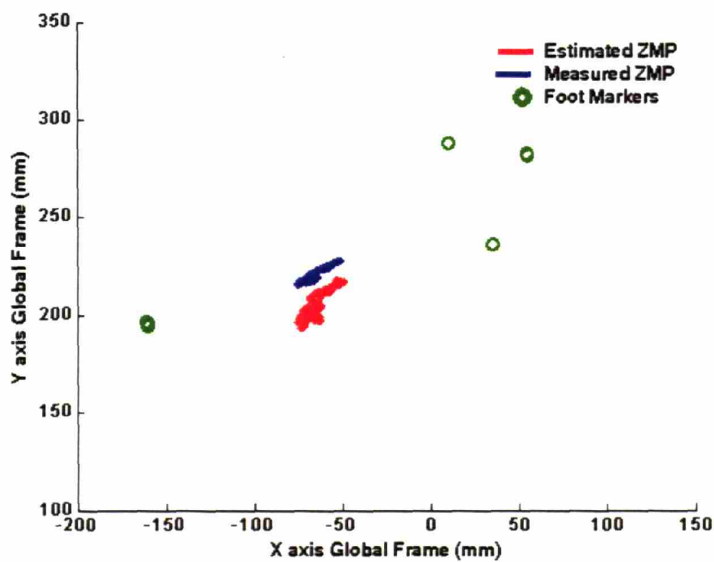
81

a)
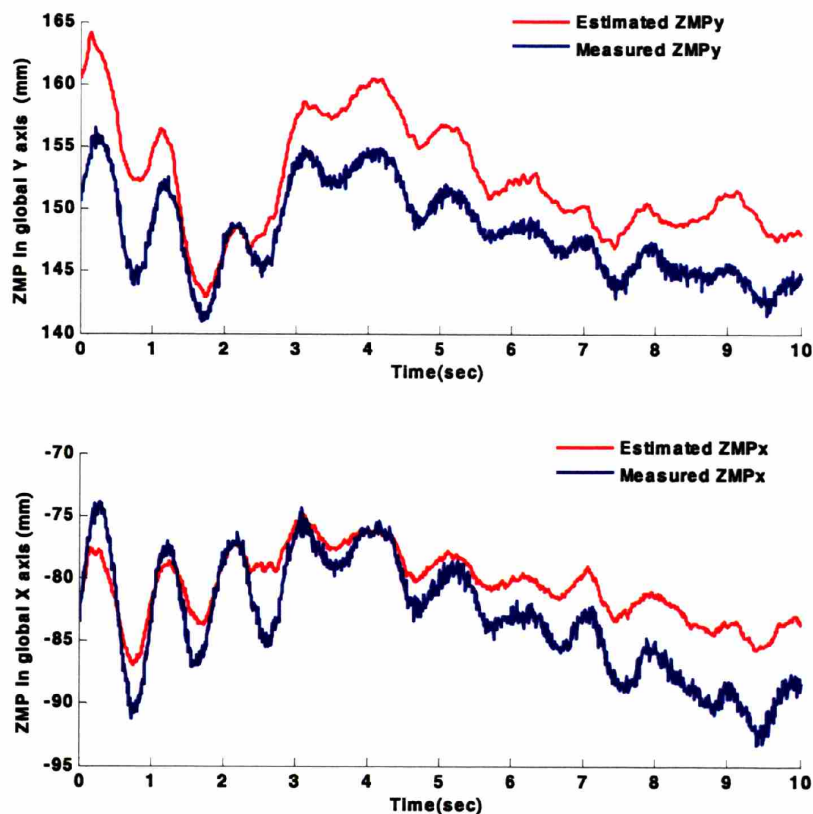
b)
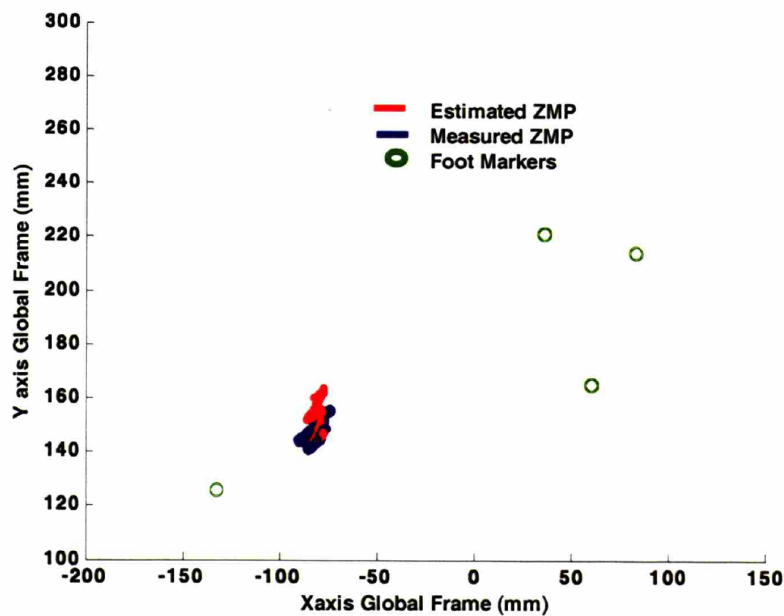
Figure 5-13. a)ZMP trajectory relative to the X and Y axis of the global coordinate frame *{G}* during quiet stance with control weight and passive ankle-foot. Single trial. b) ZMP trajectory in global coordinate frame and its relation with the foot support polygon delimited by the reflective markers.

5.7. Control Weight.- Anterioposterior Sway. Passive Ankle-Foot

| Parameter | RMS ERROR (N) | | R |
	MEAN	STDV	
FZ	1.7633	0.4752	0.9606
FY	0.7554	0.1968	0.2606
FX	7.0872	3.0834	0.2311

| Parameter | RMS ERROR (mm) | | R |
	MEAN	STDV	
ZMP Y	19.542	9.316	0.9606
ZMP X	36.933	15.125	0.9184

Average distance between estimated and measured ZMP location : 36.406 mm

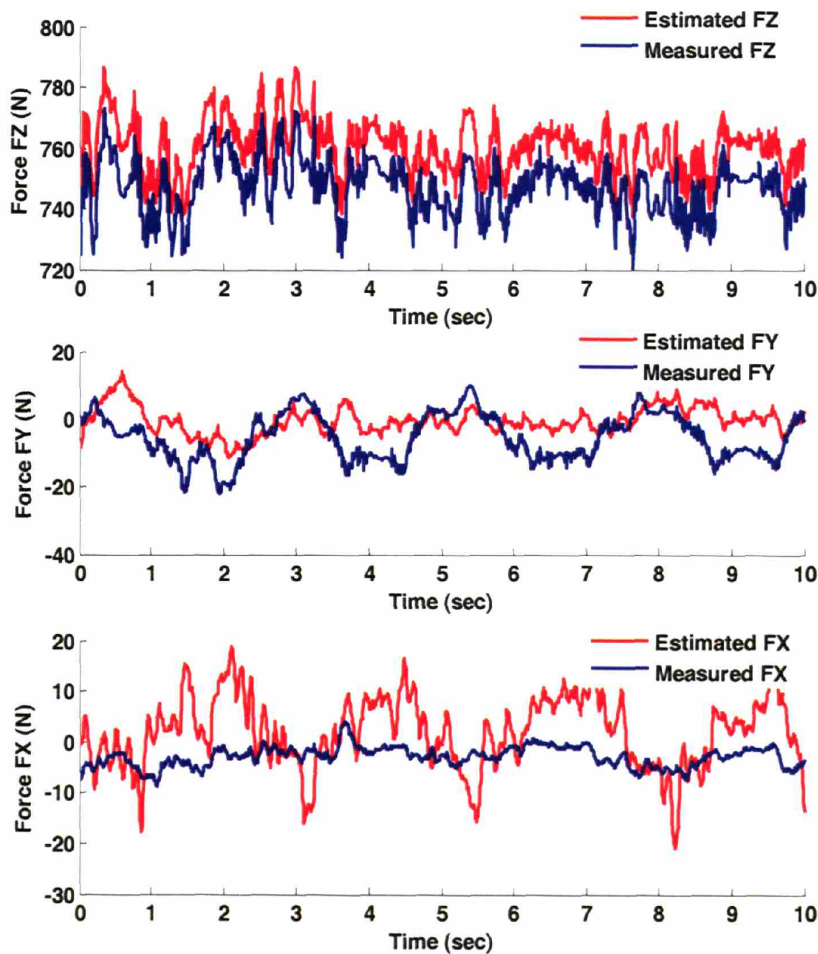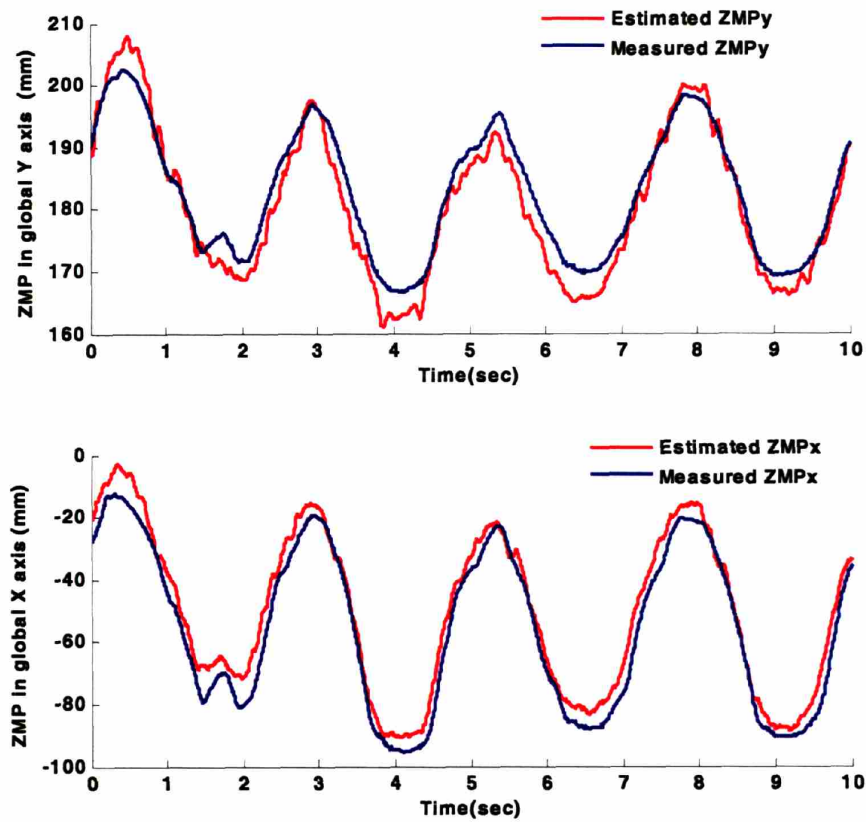**Table 5-7.** Experimental results. Control weight anterioposterior sway. Active ankle-foot
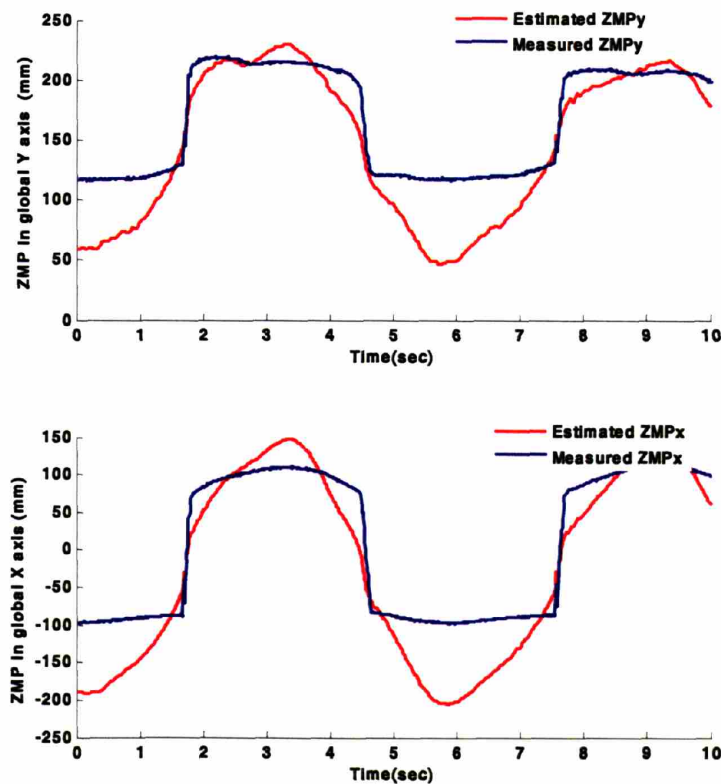
Figure 5-14. ZMP trajectory relative to the X and Y axis of the global coordinate frame *{G}*. Single trial, anterioposterior sway with control weight and passive ankle-foot

83

6   Discussion and Conclusions

In this thesis, the feasibility of estimating the GRF and the ZMP on instrumented prostheses was investigated. The use of a six-directional force-torque transducer positioned between the socket adapter and the artificial ankle structure, allowed the use of a compliant foot to be in contact with the ground. For this study a wearable computing system for the powered ankle-foot control and as an ambulatory gait analysis tool, was designed and tested. The results obtained provide interesting insights into the development of fully autonomous powered ankle-foot prostheses.

6.1.   Estimation of GRF

The observed results for the estimation of the vertical component of the GRF, when compared to the measured data, averaged a correlation factor higher than 0.9 across all experimental trials when testing with a human subject. In addition, the average RMS error was less than 5 N. The difference in the estimated and measured values of this component is primarily due to the static assumptions of the model and considering the ankle-foot as a rigid structure. No dynamic behaviors were incorporated into the model used. Furthermore, the spring like behavior of the compliant foot prosthesis, in both, active and passive devices, acts like a shock absorber for the forces interacting with the ground. In consequence, these forces are not completely sensed by the force transducer situated proximal to the ankle joint, causing a discrepancy in the estimated values. The GRF was the only external force considered to act on the ankle-foot system (assumed as a rigid body). However, there are forces interacting between the prosthesis, and the socket of the amputee subject, which were not modeled. Even though the dynamic behaviors or interactions between the prosthesis and the patient were not taken into consideration, the estimated vertical component of the GRF was highly accurate when compared to measured data given by the standard gait lab instruments. These results support the idea that during single stance support, when standing and slow walking, a static assumption is sufficient for the estimation of the vertical component of the GRF.

The estimation of the horizontal forces that act on the ground averaged a correlation factor no greater than 0.7 for all experimental trials. The best estimations were recorded during the standing and anterior-posterior sway experiments where the magnitude of the horizontal (shear) forces exerted on the ground is very small compared to the vertical component of the ground reaction force.. The interaction forces between the amputee's stump and socket are sensed by the force / torque transducer at interface between the socket and the artificial ankle. Nevertheless, these forces are not necessarily transmitted or sensed by the force platforms.

The small magnitudes of the horizontal components of the GRF, compared to the magnitude of the vertical component, reduce the influence of these values in the estimation of the ZMP location. Particularly the shear forces have very few impact on the estimations of the ZMP during the standing evaluations, were there is minimal small movement of the foot with respect to the ground.

Finally, a source of error present in the estimation of the GRF components is produced by the algebraic transformation applied to represent these values relative to the force plate reference frame. This transformation depends on the motion capture data, which normally contains noisy information. This situation was minimized by digitally filtering the recorded signals.

6.2. Estimation of ZMP

During quiet stance and anterioposterior sway experiments the amputee participant was asked to stand on one leg for a period larger than ten seconds. In order to avoid falling he was permitted to reach a support stool, used as a balance aid, located beside the force plate. When the subject reached or grabbed this balance aid, the surface of support (known as support polygon) changes, repositioning the location of the measured ZMP. In the static model employed, no other external forces besides the GRF were considered. This assumption introduced errors to the estimated values of the ZMP. Even with these considerations, the average RMS error between the estimated and measured ZMP values with the passive device (in quiet stance and anterior-posterior sway) was less than 5mm with a correlation factor higher than 0.9.

The estimation of the ZMP trajectory during the standing experiments with the passive ankle, presented better results when compared with the results of the ZMP in the active-ankle prosthesis. The fixed stiffness of the passive prosthesis and limited rotation about the ankle joint reduced the variation of the movement of the ZMP. In these trials the average distance between the estimated and measured ZMP location was less than 6 mm.

The stiffness programmed for the different trials was similar to the observed values in humans when they are standing. However, this stiffness is obviously less than of the rigid joint in the passive device. This situation allows a greater angular movement around the ankle joint in the active prosthesis. Since the subject did not have real time control of the stiffness of the ankle joint, it was more difficult for to balance on one foot. For this reason, the subject relied more on the stool as a balance aid, exerting forces not accounted for in the static model. In consequence, the support polygon changes, affecting the location of the ZMP. Even though, this circumstance affected the estimation of the ZMP for specific trials, the average distance between the measured ZMP and the value estimated by the model was small (less than 8 mm)

During the walking trials, the ZMP trajectory was estimated only during the single support phase (i.e. just one foot on the ground). Although highly correlated (R > 0.95), a constant offset average error of <10 mm was observed. This offset can further be compensated in the model during walking experiments.

The usage of a control weight did not present any advantage in the analysis as originally suspected. The reason is that this weight required the intervention of a human to avoid it falling during the experiments. This intervention results in the exertion of external forces that were not accounted for in the model. This forces incremented the area of the support disturbing the location and trajectory of the ZMP.

6.3. Contributions

In this thesis the estimation of ground reaction force components and zero moment point trajectory in instrumented ankle-foot prostheses was investigated. Using an array of embedded sensors on passive and active ankle-foot prostheses in combination with a wearable computing unit, the GRF and ZMP were estimated during standing and walking experiments. The results were compared to the values provided by standard biomechanic analysis tools such as precision force measuring platforms and 3D video motion capture system in order to validate the accuracy of the estimations.

The results of this investigation suggest that a static model can be a implemented as an estimation method for the GRF and ZMP during single leg stance phase of walking and single leg stance with passive and active prostheses. The precision of the estimations based on the static model have an average error of less than 1 cm compared to the measured values, given by precision gait laboratory instruments. This error is equal to 4% of the anterior-posterior foot length or 12% of the medio-lateral foot width.

The wearable computing system developed for this research allowed performing autonomous tests at MIT's gait lab. This system comprises a multi-purpose control and data acquisition unit that can be utilized to control and monitor, not only a robotic prosthetic but a series of sensors and actuated devices that can be worn by healthy and amputee subjects. As a general autonomous monitoring / control tool, the portable computing unit developed, is functionally flexible to be applied as an autonomous and real-time gait analysis tool for healthy and amputee population in *real life* environments.

In general, the results obtained motivate further research into bipedal locomotion, particularly in postural control for both humans and bipedal robots. In humans, developing active prostheses that use ZMP based balance controllers to improve amputee stability will represent enormous clinical benefit for lower extremity amputees. In the case of humanoid robots, the use of embedded sensors that track ZMP allowing flexible structures to be in contact with the ground will provide these machines with more human-like walking dynamics.

The work presented in this thesis intends to contribute to the development of a fully integrated artificial extremity, capable of using GRF and ZMP estimations for active balance control, that effectively mimics the behavior of the human ankle-foot complex.

7 Bibliography

Arakawa, T. & Fukuda T.1997. Natural motion generation of biped locomotion robot using hierarchical trajectory generation method consisting of GA, EP layers. *Proceedings of the IEEE Internatioal Conference on Robotics and Automation,* Albuquerque, NM. pp. 211-216.

Au, S.K., Bonato, P., Herr, H. 2005. An EMG-position controlled system for an active ankle-foot prosthesis: an initial experimental study. *ICORR 2005. 9th IEEE International Conference Rehabilitation Robotics* pp. 375 – 379.

Au, S.K., Dilworth, P., Herr, H. 2006. An ankle-foot emulation system for the study of human walking biomechanics. *ICRA 2006. Proceedings IEEE International Conference on Robotics and Automation,*May 15-19. pp. 2939 – 2945.

Balasubramaniam, R. & Wing, A. 2001. The dynamics of standing balance. *Trends in cognitive sciences.* Vol 6. No. 12. pp. 531-536.

Barnett, S., Cunningham, J., West S. 2001. A comparison of vertical force and temporal parameters produced by an in-shoe pressure measuring system and a force platform. *Clinical Biomechanics.* vol 16. pp. 353-357.

Berme, N., Lawes P., Solomonnidis S., Paul J.P. A shorter pylon transducer for measurement of prosthetic forces and moments during amputee gait. *Eng Med.* 4. pp. 6-8.

Bontrager, E.L.1998. Instrumented gait analysis systems. *In: Gait Analysis in the Science of Rehabilitation,* Department of Veterans Affairs, 2. pp. 11-32.

Buckley, J.G., O'Driscoll, D., Bennett, S.J., January 2002. Postural sway and active balance performance in highly active lower-limb amputees. *American Journal of Physical medicine & Rehabilitation.* 81(1): pp. 13-20.

Burstein, A.H., Wright, T. M., 1994. Fundamentals of orthopaedic biomechanics. *New York: Williams and Wilkins.* pp. 34.

Cavanagh, P.R. 1980. A technique for averaging center of pressure paths from force platform. *Journal of Biomechanics.* 13: pp. 397-406.

Cordero, A., Foerner, Koopman, H.J.F.M., Van der Helm, F.C.T., 2004. Use of pressure insoles to calculate the complete ground reaction forces. *Journal of Biomechanics.* 37: pp. 1427-1432.

Dasgupta, A. & Nakamura,Y. 1999. Making feasible walking motion of humanoid robots from human motion capture data. *Proceedings of the IEEE International Conference on Robotics and Automation,* Detroit, MI. pp. 47-52.

Davis, B.L. , Perry, J.E., Neth, D.C. & Waters, K.C. 1998 . A device for simultaneous measurement of pressure and shear force distribution on the plantar surface of the foot. *Journal of Applied Biomechanics.* Vol. 14. pp. 93-104.

Elftman, H. 1934. A cinematic study of the distribution of pressure in the human foot. *Anatomical Rec.* 59: pp. 481-491.

Erbatur, K., Okazaki, A., Obiya, K., Takahashi, T., Kawamura, A., 2002. A study on the zero moment point measurement for biped walking robots. *IEEE Advanced Motion Control* . Maribor, Slovenia pp. 431-436.

Ferencz, D.C., Jin, Z., Chizeck, H.J., 1993. Estimation of center-of-pressure during gait using an instrumented ankle-foot orthosis. *IEEE.* Pp. 981-982.

Gates, D.H. 2004. Characterizing the ankle function during stair ascent, descent and level walking for ankle prosthesis and orthosis design. *Master's Thesis.* Boston University.

Gatev P, Thomas S, Kepple T, and Halett M. Feedforward. 1999. Ankle strategy of balance during quiet stance in adults. *Journal of Physiology* 514: 915-928,.

Giacomozzi, C., Macalleri, V., Leardini, A., Benedetti, M.G., 2000. Integrated pressure-force kinematics measuring system for the characterization of plantar foot loading during locomotion. *Medical Biological Engineering Computing.* Vol. 38. pp. 156-163.

Goswami, A., 1999. Postural stability of biped robots and the foot rotation indicator point. *International Journal of Robotics Research* .18(6): pp. 523-533.

Goswami, A. & Kallem, V., 2004. Rate of change of angular momentum and balance maintanince of biped robots. *Proceedings of the IEEE International Conference on Robotics and Automation.* New Orleans, LA. pp. 3785-3790.

Halliday, D., Resnick, R., Walker, J., Fundamentals of physics. 5th edition. John Wiley & Sons, Inc.

Hay, J.G. 1973. Biomechanics of sports techniques. Prentice Hall, Inc., Englewood Cliffs, NJ.

Hirai, K., Hirose, M., Haikawa, Y. & Takenaka, T., 1998. The development of Honda humanoid robot. *Proceedings of the IEEE International Conference on Robotics and Automation.* Lueven, Belgium. pp. 1321-1326.

Hofmann, A., Popovic, M., Massaquoi, S., & Herr, H., 2004. A sliding controller for bipedal balancing using integrated movement of contact and non-contact limbs. *Proceedings of the IEEE/RSJ International Conference on Intelligent Robots and Systems.* Sendai, Japan. pp. 1952-1959.

Inman, V.T., Ralston, H.J., & Todd, F., 1981. Human Walking. *Baltimore:*Williams and Wilkins.

Ito, S., Aoyama, Y. & Kawasaki, H., 2003. Static balance control and external force estimation using ground reaction forces. *2nd International Symposium on Adaptive Motion of Animals and Machines.* (AMAM 2003).

Ito, S. , Kawasaki, H., 2000. A standing posture control based on ground reaction force. *Proceedings of the 2000 IEEE/RSJ International Conference on Intelligent Robots and Systems.* pp. 1340-1345.

Kinoshita, G., Kimura, T., and Shimojo, M., 2003 . Dynamic sensing experiments of reaction force distribution on the sole of a walking humanoid robot. *Proceedings of the 2003 IEEE/RSJ International Conference on Intelligent Robots and Systems.* Las Vegas, Nevada. pp. 1413-1418.

Kinoshita, G., Oota, C., Osumi, H., & Shimojo, M., 2004. Acquisition of reaction force distributions for a walking humanoid robot. *Proceedings of the 2004 IEEE/RSJ International Conference on Intelligent Robots and Systems.* Sendai, Japan. pp. 3859-3864.

Klute, G.K., Kallfelz, C.F., Czerniecki, J.M., 2001. Mechanical properties of prosthetic limbs: adapting to the patient. *Journal of Rehabilitation Research and Development. Department of Veterans Affairs.* Vol. 38 No. 3. pp. 299-307.

Kudoh, S., 2004. Balance maintenance for human-like models with whole body motion. *Ph.D. Thesis,* University of Tokyo.

Lawrence, T., Schmidt, L., R., N., 1997. Wireless In-Shoe Force System. *Proceedings 19th International Conference IEEE Engineering in Medicine and Biology Society.* Chicago, IL. pp. 2238-2241.

Loram, I.D., & Lakie, M., 2002. Direct measurement of human ankle stiffness during quiet standing: the intrinsic mechanical stiffness is insufficient for stability. *Journal of Physiologiy.* vol. 545. pp. 1041-1053.

Miller, W.C., Deathe, A.B., 2004. A prospective study examining balance confidence among individuals with lower limb amputation. *Disability Rehabilitation.* Jul 22-Aug.5: 26(14-15): pp. 875-81.

Morasso, P. & Sanguinetti, V., 2001. Ankle muscle stiffness alone cannot stabilize balance during quiet standing. *Rapid Communication Journal of Neurophysiology.* 88: pp. 2157-2162.

Morimoto, S. Evaluation of foot ankle units by an ambulatory gait measuring system. *Proceedings of the 7ᵗʰ World Congress of the International Society for Prosthetics and Orthotics (ISPO).* Chicago. Vol. II. pp. 323

Morris, S.J., Paradiso, J.A., 2002. Shoe-integrated sensor for wireless gait analysis and real-time feedback. *Proceedings of the Second Joint EMBS/BMES Conference.* October. pp. 2468-2469.

Napoleon, S. Nakaura & Sampei, M., 2002. Balance control analysis of humanoid robot based on ZMP feedback control. *IEEE Proceedings of the. International Conference on Intelligent Robots and Systems.* Lausanne, Switzerland. pp. 2437-2442.

Nigg, B.M. & Herzog, W. Biomechanics of the musculo-skeletal system. 1994. John Wiley & Sons Inc.

Nishiwaki, K., Murakami, Y., Kagami, S., Kuniyoshi, Y., Inaba, M., Inoue H., 2002. A six-axis force sensor with parallel support mechanism to measure ground reaction force of humanoid robot. *Proceedings of the 2002 IEEE International Conference on Robotics & Automation.* Washington, DC. pp. 2277-2282.

Nordin & Frenkel. 2001. Basic biomechanics of the musculoskeletal system. 3ʳᵈ ed. Williams & Wilkins.

Palmer, M., 2002. Sagittal plane characterization of normal human ankle function across a range of walking gait speeds. *Master's Thesis.* Massachusetts Institute of Technology.

Park, J.H. & Rhee, Y.K.,October 1998. ZMP Trajectory generation for reduced trunk motion of biped robots. *Proceedings IEEE/RSJ International. Conference in Intelligent Robots and Systems*, IROS ' 98. pp. 90-95.

Perry, J.1992. Gait analysis normal and pathological function. Slack, Inc. Thorofare, NJ.

Pitkin, M., et al. 2002. Biomechanics of ice hockey skating in amputees with foot and ankle prostheses. *In 7th Annual Russian National Congress.*.St. Petersburg, Russia.

Pitkin, M., Quesada, P.M., Colvin, J., Hays, J. & White, C., 1999. moment of resistance in the prosthetic feet as possible predictor of patient's   performance and comfort. *25th Academy Annual Meeting and Scientific Symposium, American Academy of Orthotists and Prosthetists.*

Popovic, M., and Herr, H. 2005. Global motion control and support base planning. *Proceedings of the IEE/RSJ International Conference on Intelligent Robots and Systems,* Alberta, Canada.

Popovic, M. B., Goswami, A. & Herr, H., 2005. Ground reference points in legged locomotion: definitions, biological trajectories and control implications. *International Journal of Robotics Research .*Vol. 24. No. 12. pp. 1013-1032.

Pratt, G.A., Williamson, M.M., 1995. Series elastic actuators. *Proceedings on IEEE/RSJ International Conference on Intelligent Robots and Systems.* Pittsburgh, PA. pp. 399-406.

Qinghua, L., Takanashi, Atsuo & Kato, Ichiro. 1992. Development of ZMP measurement system for biped walking robot using universal force-moment sensors. *Journal of Robotics Society of Japan.* Vol. 10. No.6. pp. 828-833.

Razian, A.M. & Pepper, M. G., September 2003. Design, development, and characteristics of an in-shoe triaxial pressure measurement transducer utilizing a single element of piezoelectric copolymer film. *IEEE Transactions on Neural Systems and Rehabilitation Engineering.*Vol. 11. No. 3 . pp. 288-293.

Sanders, J.E. ,Miller, R. A., Berglund, D.N., Zachariah, S.,1997. A modular six-directional force sensor for prosthetic assessment: a technical note. *Journal of Rehabilitation Research and Development.* Vol. 34. no. 2. pp. 195-202.

Sanders, J.E., Daly, C.H., Cummings, W.R., Reed, R.D., Marks, R.J., 1994. A measurement device to assist amputee prosthetic fitting. *Journal of Clinical Engineering.* Vol. 19(1): pp. 63-71.

Sardain, P. & Bessonnet, G. 2004. Forces acting on a biped robot. Center of pressure-zero moment point. *IEEE Transactions on Systems, Man and Cybenetics.*
Part A. 34(5): pp. 630-637.

Saunders, J.B.D.M., Inman, V.T., Eberhart. H.S.,1953. The major determinants in normal and pathological gait. *Journal of Bone and Joint Surgery.* 35A:
pp. 543-558.

Savelberg, H.H.C.M., De Lange, A.L.H. 1999. Assessment of the horizontal, for-aft component of the ground reaction force from insole pressure patterns by using artificial neural networks. *Clinical Biomechanics.* Vol 14. pp. 585-592.

Shimba, T., 1984, An estimation of center of gravity from force platform data. *Journal of Biomechanics.* 17 (1): pp. 53-60.

Soutas-Little, R.W.,1990.Center of pressure plots for clinical uses. *Biomechanics of normal and proshtetic gait, ASME, BED.*Vol.4. DSC-Vol. 7: pp. 69-75.

Tak, S., Song, O. & Ko, H.S. 2000. Motion balance filtering.*Eurographics* 2000.
Vol. 19. No. 3.

Takahashi, Y., Kagami, S. , Ehara, Y., Mochimaru, M., Takahashi, M., Mizoguchi, H., 2004. Six-axis force sensing footwear for natural walking analysis. *IEEE International Conference on Systems, Man and Cybernetics*. pp. 5374-5379.

Veltink, P.H., Liedtke, C., Droog, E., Van der Kooij, H., 2005. Ambulatory measurement of ground reaction forces. *IEEE Transactions on Neural Systems and Rehabilitation Engineering.* Vol 13. No. 3. pp. 423 – 427.

Vukobratovic, M. & Juricic, D.1969. Contribution to the synthesis of biped gait. *IEEE Transaction on Biomedical Engineering.* Vol. 16. No. 1. pp.1-6.

Vukobratovic, M. & Stepanenko, J. 1972. On the stability of anthropomorphic systems. *Mathematical Biosciences.* Vol. 17. pp. 1-37.

Vukobratovic, M. & Borovac, B., 2004.Zero-moment point—thirty five years of its life. *International Journal of Humanoid Robotics.* Vol. 1. No. 1. pp. 157-173.

Whittle, M.W., 1991. Gait analysis: an introduction. 3rd ed. Oxford: Butterworth-Heinemann.

Williams, R.B., Porter, D., Roberts, V.C. & Rega, J.F., 1992. Triaxial force transducer for investigating stresses at the stump/socket interface. *Medical & biological engineering & computing.* Vol 30. pp. 89-96.

Winter, D., 1984 Kinematic and kinetic patterns in human gait. *Human Movement Science.* Vol. 3. pp. 51-76.

Winter, D.A.,1987. The biomechanics and motor control of human gait. Waterloo: University of Waterloo press.

Winter, D.A.,1995. Gait & Posture. 3rd ed. pp.193-214.

Winter, D.A., Patla A.E., Prince F., Ishac, M., Perczak, K., 1998. Stiffness control of balance in quiet standing. *Journal of Neurophysioogy* .80(3): pp. 1211-21.

Winter, D. A. Patla, A. E. , Rietdyk S. & Ishac, M.G., 2001. Ankle muscle stiffness control of balance in quiet standing. *Journal of Neurophysiology.* 85: pp. 2630-2633.

Zhang K., Sun, M. , Lester, D. K. , Pi-Sunyer, F. X. , Boozer, C. N., Longman, R. W., 2005. Assessment of human locomotion by using an insole measurement system and artificial neural networks. *Journal of Biomechanics.* Vol 38. Issue 11. pp. 276-2287.

Zhiming, J., Findley, T., Chaudhry, H. , Bukiet B. 2004 . Computational method to evaluate ankle postural stiffness with ground reaction forces. *Journal of Rehabilitation Research and Development.* Vol. 41. No. 2 pp. 207-214.

http://www.bourns.com

http://www.kwon3d.com/ Author: Young-Hoo Kwon, 1998.

http://kwon3d.com/theory/grf/cop.html

http://world.honda.com/ASIMO/history/technology2.html

http://www.maxonmotor.com

http://www.monash.edu.au

http://www.motionanalysis.com

http://www.novel.de

http://www.ossur.com

http://www.tekscan.com

http://www.usdigital.com

http://www.vicon.com